

ABSTRACT

Title of Document: Assessment of Duct Leakage Rates on Stairwell Pressurization System

Jerry Richard Taricska, BSCE., 2014

Directed By: Professor James A. Milke
Department of Fire Protection Engineering

This study aims to evaluate the effects duct leakage had on a stairwell pressurization system in a high-rise residential building by using a network model, CONTAM. The network model was used to determine if the pressurized system was capable of being balanced and perform as intended during a fire incident. The subject building had two stairwells, each fed by a fan located on the 2nd and 29th floors of a 31-story building. Each fan fed a multi-injection duct system which ran through a mechanical shaft located next to each stairwell. This study evaluated the effects that building leakages and temperatures (stack effect) had on air leakage out of the duct system by comparing fan capacities to stairwell pressurization requirement. CONTAM was used to simulate these effects by running both a duct balance method and steady state method. The results from this study determined that as duct leakage rates increased, fan capacities increased to meet the stairwell pressurization requirements for a high-rise building. Additionally, the results determined that the building leakage and exterior temperatures increased the air flow leaking out of the duct system.

ASSESSMENT OF DUCT LEAKAGE RATES ON STAIRWELL
PRESSURIZATION SYSTEM

By

Jerry Richard Taricska

Thesis submitted to the Faculty of the Graduate School of the
University of Maryland, College Park, in partial fulfillment
of the requirements for the degree of
Master of Science
2014

Advisory Committee:
Professor James A. Milke, Chair
Professor Andre Marshall
Professor Michael J. Gollner

© Copyright by
Jerry Richard Taricska
2014

Dedication

I dedicate this degree to my father, Dr. Jerry Robert Taricska whose continued support and counsel enabled me to complete this process. Also in loving memory of my grandparents who understood the importance of education; Paul Dolenc and Antonia Iglic Dolenc, Slovenian descent and Charles Taricska and Emma Orosz Taricska, Hungarian and Romanian descents.

Acknowledgements

First and foremost, I wish to express my sincere thanks to my advisor and committee members, Dr. Milke, Dr. Marshall, and Dr. Gollner. It was their support, guidance, encouragement, and insight that made this thesis possible and I am grateful for the opportunity to have worked with them.

I would like to thank Steven Stregre for his support, time and insight on developing my CONTAM model. I would also like to thank Michael Ferreira for his time and guidance.

Finally, and with gratitude, I want to thank my family, whose love, support and encouragement has guided me through my graduate program. Thanks go to my father, Jerry Taricska, my mother, Josephine Dolenc Taricska, and my four sisters, Jaclyn, Julie, Jillian and Joyce. I am most grateful for all their prayers, time, help and advice.

Table of Contents

Dedication	ii
Acknowledgements.....	iii
Table of Contents	ii
List of Tables	vii
List of Figures	viii
Chapter 1: Introduction	1
1.1 Objective.....	5
Chapter 2: Literature Survey.....	6
2.1 Duct Leakage:	6
2.2 Stack Effect.....	7
2.3 Building Leakages	8
2.4 CONTAM.....	9
2.4.1 Duct System.....	10
Chapter 3: Building Floor Plan Layout.....	15
3.1 Leakage Building Floor Plans.....	15
3.2 CONTAM Building Layout.....	16
3.3 Duct Layout	17
Chapter 4: CONTAM Inputs	20
4.1 Global Inputs.....	20
4.1.1 Ducts System	20
4.1.2 Airflow Paths Types	23
4.1.3 Doors.....	25

4.1.4 Zones.....	25
4.1.5 Density.....	26
4.2 Changeable Variables.....	29
4.2.1 Duct Leakage Rates.....	30
4.2.2 Building Components.....	30
4.2.3 Weather.....	32
4.2.3 Simulation Methods.....	34
Chapter 5: Calibration.....	35
5.1 Duct Balance Simulation Methods.....	35
5.2 Steady State Simulation Methods.....	36
5.3 Calibration Results.....	37
Chapter 6: Data Analysis and Discussion.....	40
6.1 Steady State Simulation Method – Stairwell_A and Shaft_A.....	40
6.1.1 Stairwell_A Data Analysis:.....	41
6.1.2 Shaft_A Data Analysis:.....	43
6.1.3 Summary:.....	46
6.2 Duct Balance Simulation Method – Stairwell_A and Shaft_A.....	48
6.2.1 Stairwell_A Data Analysis:.....	48
6.2.2 Shaft_A Data Analysis:.....	50
6.2.3 Summary:.....	53
6.3 Steady State Simulation Method – Stairwell_B and Shaft_B.....	55
6.3.1 Stairwell_B Data Analysis:.....	55
6.3.2 Shaft_B Data Analysis:.....	57

6.3.3 Summary:.....	60
6.4 Duct Balance Simulation Method - Stairwell_B and Shaft_B.....	62
6.4.1 Stairwell_B Data Analysis:.....	62
6.4.2 Shaft_B Data Analysis:.....	64
6.4.3 Summary:.....	67
6.5 Single-Injection and Simple Air-Handle System Comparison:	69
Chapter 7: Conclusion.....	73
Chapter 8: Suggestions for Further Study.....	76
Appendix A.....	77
Appendix B	84
Duct Balance Simulation Method.....	84
Steady State Simulation Method.....	90
Bibliography	97

List of Tables

Table 1: CONTAM Sketchpad Icons (shown in default colors) [5].....	16
Table 2: Building leakage rates for tight and loose leakage	31
Table 3: Shows the location of where the minimal door pressure difference of 0.10 inches of H ₂ O for each model.....	38
Table 4: Summary of Stairwell_A fan capacity for steady state simulation.....	47
Table 5: Summary of Stairwell_A fan capacity for duct balance simulation	54
Table 6: Summary of Stairwell_B fan capacity for steady state simulation.....	61
Table 7: Summary of Stairwell_B fan capacity for duct balance simulation	68
Table 8: Fan capacity for high-rise building with single injection system and simple AHS system	70
Table 9: Fan capacity for high-rise building with single injection system and simple AHS system	72

List of Figures

Figure 1: Arrows indicated air leaking out of the duct system	3
Figure 2: Leakage drawing of the 7th through 17th floors showing location of stairwells and duct shafts.	15
Figure 3: CONTAM model of the ground floor	17
Figure 4: CONTAM model of the 29th floor.....	17
Figure 5: Isometric of Stairwell A and Shaft A with duct segments.	19
Figure 6: Isometric of Stairwell B and Shaft B with duct segments.....	19
Figure 7: Duct sizes and fan location from Basement level to Roof used in the CONTAM models.....	22
Figure 8: One variation of model simulation that produces 12 models	29
Figure 9: Duct leakage rate vs fan capacity for Stairwell_A running a steady state simulation for loose and tight building leakage.....	42
Figure 10: Outside weather conditions vs fan capacity for Stairwell_A. Running steady state method.....	42
Figure 11: Airflow leakage from junction throughout Shaft_A during winter weather conditions for steady state simulation.....	44
Figure 12: Airflow leakage from junction throughout Shaft_A during summer weather conditions for steady state simulation.	45
Figure 13: Airflow leakage from junction throughout Shaft_A during standard temperature for steady state simulation.	46
Figure 14: Duct leakage rate vs fan capacity for Stairwell_A running a duct balance simulation for loose and tight building leakage.....	49

Figure 15: Outside weather conditions vs fan capacity for Stairwell_A. Running duct balance method	49
Figure 16: Airflow leakage from junction throughout Shaft_A during summer weather conditions for duct balance simulation.....	51
Figure 17: Airflow leakage from junction throughout Shaft_A during standard temperature (20°) for duct balance simulation.....	52
Figure 18: Airflow leakage from junction throughout Shaft_A during winter temperature (-20°) for duct balance simulation.	53
Figure 19: Duct leakage rate vs fan capacity for Stairwell_B running a steady state simulation for loose and tight building leakage.....	56
Figure 20: Outside weather conditions vs fan capacity for Stairwell_B. Running steady state method.....	56
Figure 21: Airflow leakage from junction throughout Shaft_B during winter temperature (-20°C) for steady state simulation.	58
Figure 22: Airflow leakage from junction throughout Shaft_B during summer temperature (40°C) for steady state simulation.	59
Figure 23: Airflow leakage from junction throughout Shaft_B during standard temperature (20°C) for steady state simulation.	60
Figure 24: Duct leakage rate vs fan capacity for Stairwell_B running a duct balance simulation for loose and tight building leakage.....	63
Figure 25: Outside weather conditions vs fan capacity for Stairwell_B. Running duct balance method	63

Figure 26; Airflow leakage from junction throughout Shaft_B during summer temperature conditions for duct balance simulation.	65
Figure 27: Airflow leakage from junction throughout Shaft_B during standard temperature for duct balance simulation.	66
Figure 28: Airflow leakage from junction throughout Shaft_B during winter temperature for duct balance simulation.	67

Chapter 1: Introduction

Many people today may have difficulties continually traveling down 30 flights of stairs, and nearly impossible for those with mobility impairments and wheel chairs users. Jeffery Tubbs, Matthew Johann and Andrew Neviackas discussed the life safety approach to smoke control for tall buildings. They also discussed the importance of developing and incorporating a smoke management system into a comprehensive life safety programs. [1]

In building fires, smoke is recognized as the major killer by containing toxic gases, heating the surrounding environment and reducing visibility [2] [3]. Stairwells are used as a means of egress during the time of evacuation. Pressurized stairwells inhibit smoke from entering the stairwell. Pressurized stairwells are mechanically pressurized, either by a single injection system or by a multiple-injection system, with outside air to keep smoke from contaminating the stairwell during a fire incidence. These systems contained a fan that supplied air to a duct system, which is not airtight causing the fan to be ineffective. Field tests done by Yanling Wang and Fuseng Gao in Harbin, Heilongjian Province, China demonstrate that not all smoke control systems in high-rise buildings ensure safe evacuation. [4]. Either under sizing or oversizing a fan capacity for a pressurization system can hinder occupants from evacuating safely. Yanling Wang and Fuseng Gao discussed the importance of designing a system from over pressurizing.

Industry designers will consider exterior temperature and building leakage when designing a stair pressurization system. The industry designer will either consider a single fan located on the top of the building or a single fan located at the bottom of the stairwell and another one located on the top of the stairwell. These two pressurization systems are limited and don't consider the effects of how much air flow is lost due to inadequate duct construction.

An analysis of stairwell pressurization system was done using CONTAM, which is computer program. This program provides multizone air quality and ventilation analyses that determine infiltration, exfiltration, and room-to-room airflows in building systems driven by mechanical means. The program also examines the affect air buoyancy when conditions create difference between the indoor and outdoor air temperature. [5]

This research focused on a 105 meter tall building with two stairwells pressurized by a multiple-injection system. This building design was chosen to assess how different floor layouts effect the air movement within the building. The multiple-injection system consisted of two supply fans located on the 2nd and 29th floors of a 31-story building. Each fan was fed by a multi-injection duct system, which runs through a mechanical shaft located next to each stairwell. Each stairwell and pressurization system was assessed separately due to their location in the building. One stairwell was located in the center of the building with four walls exposed to indoor temperature,

whereas the other stairwell was located in the corner of the building with two walls exposed to outdoor temperature and two walls exposed to indoor temperature.

This study focused on assessing the affects of different duct leakage rates by comparing fan capacities needed to pressurize a stairwell. Four different duct leakage rates were evaluated: two sealed rates at 0.14 L/s/m^2 , and 0.62 L/s/m^2 , and two unsealed rates at 2.48 L/s/m^2 , and 5.6 L/s/m^2 . [6] These values influenced the fan capability to efficiently pressurize the stairwell. Sealed ducts were considered to have less leakage than the unsealed ducts due to the fabricating machinery used, material thickness, assembly methods, and installation workmanship. A rectangular duct is shown in Figure 1, the image show arrows at each joint connection where air leaks out of the duct system due to inadequate fabrication or construction. The American Society of Heating, Refrigeration and Air-Conditioning Engineers suggested that unsealed metal ducts with longitudinal seams account for 10 to 15% of the total duct leakage [6].

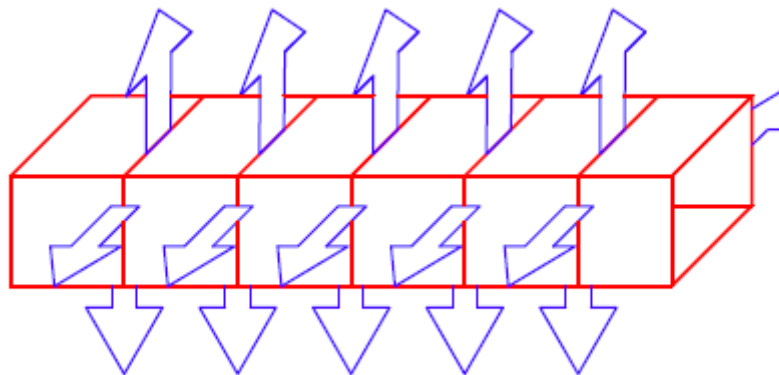


Figure 1:Arrows indicated air leaking out of the duct system to surrounding

Additionally, this study examined the effect of temperatures (stack effect), building leakages and two simulation methods on airflow requirements to pressurize the stairwells. These conditions altered the air movement through ducts and throughout the building affecting the amount of air needed to pressurize the stairwell.

This research evaluated the change in exterior temperatures of -20°C and 40°C , while interior building temperature stayed at a constant 20°C . The due to the difference between interior and exterior temperature is called stack effect, the vertical air movement within a building driven by buoyancy. The high rise building has a high pressure difference between the bottom and the top floors, which tends to move smoke or air to the upper floors in winter conditions. These temperatures were chosen to examine the weather conditions that can affect the air movement in a high-rise building.

The building leakages evaluated the movement of air through cracks, walls, floors, and door cracks. These building leakages varied, because of the types of material used to construct the building. With a tight building leakage less air flows between zones within the building, reducing the amount of air required to pressurize the stairwell. While loose building leakage allowed more air flow between zones within the building, an increased quantity of air is required to pressurize the stairwell.

This research examined two simulation methods to assess which one more accurately replicated changing variables. Each simulated model was calibrated to a minimal door

pressure difference of 0.10 inches of water to meet the National Fire Protection Association standard requirement [7].

1.1 Objective

The objective of this research was to provide a comprehensive evaluation of the effects of duct leakage on stairwell pressurization systems in a high-rise building. This research evaluated the minimal fan capacities needed to pressurize stairwells and evaluated parameters that influenced fan performance. It also evaluated the influence of air movement on each stairwell and each mechanical ventilation shaft location. Finally, this research evaluated the performance of steady state and duct balance simulation methods.

Chapter 2: Literature Survey

Previous research was done separately on duct leakage rates, stack effect and building leakage. This research evaluated the ability to simulate duct leakage on a stairwell pressurization system for a high-rise building by examining the affects temperature, building leakage and simulation methods. The importance of each of these factors is further discussed below.

2.1 Duct Leakage:

The airflow leaking out of the duct system affects the total fan capacity required to pressurize the stairwell or the airflow leakage between the stairwell and mechanical shaft. The duct leakage values come from research done in 1972 by the American Iron and Steel Institute (AISI) and Sheet Metal and Air Conditioning Contractors' National Association, INC. (SMACNA) the measured and analyzed leakage rates from seams and joints [8] and in 1995 by Swim and Griggs who developed a duct leakage measurement system to measure the total leakage rates and the leakage of the joints and seams. [9] These results are summarized in the American Society of Heating, Refrigeration and Air-Conditioning Engineers (ASHRAE). The airflow rate through a duct leak is a function of pressure difference between the surrounding space and the duct, Equation 1. [6]

$$Q = C \Delta P_s^N$$

Equation 1

where:

Q = leakage rate, L/(s m²)

C = reflective duct insulation area, (1/m²)

ΔP_s = static pressure differential from duct interior to exterior, Pa

N = exponent relating to turbulent or laminar flow in leakage path

2.2 Stack Effect

Stack effect causes the vertical air movement within a building driven by buoyancy, due to a difference between interior and exterior temperature. A high rise building has a high pressure difference between the bottom and the top floors, which tends to move smoke to the upper floors. The buoyancy of warm gases drives the smoke upward through any openings in the building. Maatouk Khouhi's study on airflow movement through a building enclosed during winter temperature conditions found that an "upward air movement current inside the building, with air flowing into vertical shafts from the lower floors and out to the upper ones." [10]. Erik Anderson showed that building height increases the stack effect conditions in a building. [11] The pressure difference due to buoyancy is calculated using Equation 2 [7]

$$\Delta P = 3460 \left[\frac{1}{T_o} - \frac{1}{T_F} \right] h$$

Equation 2

Where

ΔP = Pressure difference due to buoyancy, Pa

T_o = absolute temperature of surrounding, K

T_F = absolute temperature of outside, K

h = distance above neutral plane, m

When the outside air temperature is less than the building temperature, an upward airflow frequently moves from the bottom to the upper floors. This air movement occurs in mechanical shafts, stairwells, linen shaft, plumbing shafts and elevator shafts. The rising air reduces the pressure below the buildings neutral plan, drawing in cold air in through cracks, open doors, or other leakages points. This upward air movement is caused by the buoyancy of warm air relative to the cold outside air. When the outside air temperature is warmer than the temperature within the building the cooler air moves downward within the building shafts. This is called reverse stack effect.

2.3 Building Leakages

An analysis of the building leakage assesses the amount of airflow leaking through the building interior and exterior walls, and floors. The amount of airflow passing each component depends on how well the building was constructed resulting in an analysis of the two extremes, tight and loose building leakage. A tight building leakage has less airflow passing through cracks or openings in walls and floors, while loose building leakage has a greater amount of air passing through them. Tight, average and loose

building leakages for exterior building walls, stairwell walls, elevator walls and floors come from field results done by Tamura and Wilson in 1966, Tamura and Shaw from 1976 to 1978 and more recently by Shaw, Reardon and Cheung in 1993. There results for building leakage are summarized in the Handbook of Smoke Control Engineering [2].

The air movement in the building affects how the duct system operates either by increasing/decreasing the pressure in the duct shaft which affects the air leaking out of the duct or creating an increase or decrease in pressure difference between zones which affects the fan capacity needed to pressurize the stairwell. Andrew Persily suggests that *“taller buildings may be tighter because the type of leakage seen in these buildings”* [12]. This would suggest a smaller fan size required to pressurize the stairwell and the airflow in the building would have less of an impact on the duct system.

2.4 CONTAM

An analysis of stairwell pressurization system is done using CONTAM, which is a multizone air quality and ventilation analysis computer program designed to determine: infiltration, exfiltration, and room-to-room airflows in building systems driven by mechanical means, and buoyancy effects induced by the indoor and outdoor air temperature difference. [5] The CONTAM analysis considers temperature and building leakage affect duct leakage.

CONTAM has two types of mechanical air supply/exhaust systems; a simple air-handling system (AHS) and detailed duct system. The AHS is a simple way to utilize supply/exhaust systems into a building without having to construct and to define an entire duct system. This system has three implicit flow paths: (1) recirculation, (2) outdoor and (3) exhaust. The AHS does not take into account the leakage flow out of the duct system.

This simulation used a detailed rectangular duct system that requires the following parameters: duct size (width, height), length of each duct segment, roughness, and leakage rate at static pressure of 250 Pa. A duct segment is accompanied at each end by either a junction and/or a terminal point that also require additional information. For each duct size a new *duct flow element* was created. CONTAM user manual states: “*Duct flow elements* describe the mathematical relationship between flow through and pressure drop along the duct, the flow resistance or forced flow characteristics, cross-sectional geometry, and optional leakage per unit length of a duct.” [5]

2.4.1 Duct System

CONTAM has four *duct flow element* types that can be chosen to determine the airflow and leakage:

- Power law Model: Orifice Area,
- Power law Model: $F = C(\Delta P)^n$ is a mass flow model,
- Power law Model: $Q = C(\Delta P)^n$ is a volumetric flow model, and
- Darcy-Colebrook model.

To describe airflow through an orifice, the Power law Model: Orifice Area presented as Equation 3, allows for input of the cross-sectional area (A), and discharge coefficient (C_d), and flow exponent.

$$Q = C_d A \sqrt{\frac{2\Delta P}{\rho}} \quad \text{Equation 3}$$

Where:

Q = volumetric flow rate, m³/s

C_d = discharge coefficient, dimensionless

A = cross-sectional area, m²

ΔP = pressure difference, Pa

ρ = density, kg/m³

The Darcy-Colebrook model is a combination of Darcy-Weisbach and Colebrook's equations, the most commonly model used to calculate the fluid flow in each conduit (duct segment), considering the total pressure change and the duct friction factor. The Darcy-Weisbach relation is used to calculate pressure loss in duct due to friction by Equation 4. [13]

$$\Delta p_f = f \frac{L}{D_h} \times \frac{\rho V^2}{2} \quad \text{Equation 4}$$

Where

Δp_f = pressure loss in duct due to friction, Pa

f = friction factor of duct, dimensionless

L = duct length, m

D_h = hydraulic diameter, m

V = average velocity inside duct, m/s

The hydraulic diameter is four times the duct area divided by the perimeter of the cross section. The dynamic pressure loss due to elbows, transitions, fittings, and junctions are determined by Equation 5. [5]

$$\Delta p_d = C_d \frac{\rho V^2}{2} \quad \text{Equation 5}$$

Where

Δp_d = dynamic pressure loss in duct due, Pa

C_d = dynamic loss coefficient (elbows, transitions, fittings and junctions each have unique C_d value.)

The total pressure change for the duct system is calculated by the pressure loss due to friction and the sum of the dynamic loss in the system. See Equation 6. [5]

$$\Delta P = \Delta p_f + \sum \Delta p_d \quad \text{Equation 6}$$

Where

ΔP = total pressure loss, Pa

The nonlinear Colebrook equation calculates the friction factor which depends on the flow regime and the geometry of the duct segments, Equation 7 [14]

$$\frac{1}{\sqrt{f}} = 1.44 + 2 \log\left(\frac{D_h}{\varepsilon}\right) - 2 \log\left(1 + \frac{9.3}{Re\left(\frac{D_h}{\varepsilon}\right)\sqrt{f}}\right) \quad \text{Equation 7}$$

Where

ε = roughness dimension, mm

Re = Reynolds number, dimensionless

This nonlinear Colebrook equation is currently used in CONTAM 3.1 to determine friction losses in a section of duct. The Reynolds number relates fluid flow with velocity, density, viscosity and hydraulic geometry as shown in Equation 8. [5]

$$Re = \frac{\rho V D_h}{\mu} \quad \text{Equation 8}$$

where

μ = dynamic viscosity (kg/(m s))

D_h = hydraulic Diameter (m)

Mass flow can be related to the Reynolds number by using $F = \rho VA$ which gives Equation 9

$$Re = \frac{FD_h}{\mu A} \quad \text{Equation 9}$$

CONTAM uses Equation 10 to determine airflow in a duct system by using the friction factor from Colebrook's equation and the total pressure difference that includes the Darcy-Weisbach's pressure difference due to friction.

$$F = \sqrt{\frac{2\rho A^2 \Delta P}{fL/D_h + \sum C_d}} \quad \text{Equation 10}$$

Where:

$$\sum C_d = \text{sum of dynamic loss coefficient}$$

The Darcy-Colebrook's method only requires an input of the duct roughness factor, duct size and duct leakage rate to determine the pressure difference, flow rate, velocity of air and airflow direction for each duct segment.

Chapter 3: Building Floor Plan Layout

The detailed leakage floor plans for a 31 story building were used to replicate the residential building in the CONTAM Model so that forced air duct systems could be modeled as a specific case study for the pressurization of the stairwells.

3.1 Leakage Building Floor Plans

The residential building has different floor plans for different floor levels. The building contains one basement level with partitions that contain 16 rooms, six floors with an open floor layout, 24 floors with partitions that contains 321 bedrooms and 321 bathrooms. The six open floor plans consist of a lobby floor, two restaurant floors, and three mechanical floors.

The 31 story building has a total elevation of 104.9 m with floor heights ranging from 2.95 m to 6.71 m shown in **Appendix A**. A typical floor plan is shown in Figure 2 depicting 26 rooms, two stairwells, four elevator shafts, and 23 mechanical shafts. The remaining floor plan layouts are presented in **Appendix A**.

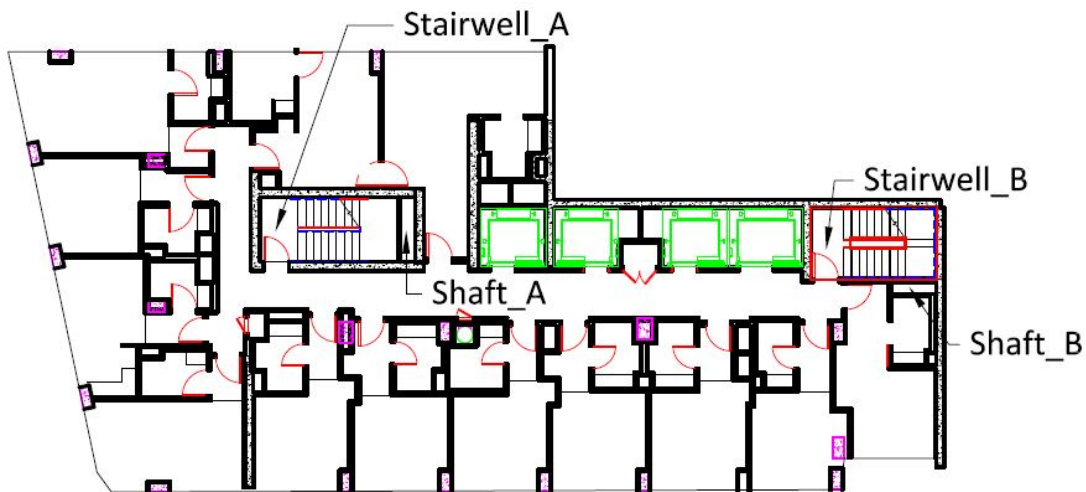


Figure 2: Leakage drawing of the 7th through 17th floors showing location of stairwells and duct shafts.

The building floor plan show Shaft_A on the right side of Stairwell_A located on the upper left side of the floor plan and Shaft_B on the lower side of Stairwell_B located on the upper right side of the floor plan. Additionally, the floor plan shows the location of four elevator shafts, mechanical exhaust shafts, mechanical supply shafts, plumbing shaft, and one linen shaft. The elevator shafts, linen shaft, both stairwells and supply shaft continued to the roof level.

3.2 CONTAM Building Layout

The leakage floor plans were used to construct a CONTAM model for the analysis.

Table 1 presents the icons used in the CONTAM model to depict walls, zones, duct components, and airflow paths.

Table 1: CONTAM Sketchpad Icons (shown in default colors) [5]

Icon Category	Component Icons
Walls	
Zones	
Duct Segments	
Duct Junctions	
Duct Terminals	
Simple AHS	
Airflow Paths	

The CONTAM building components were used to simulate spaces in each floor plan.

The geometry of each floor along with stairwells were drawn into the CONTAM model to replicate the residential building. Within each enclosed region is a single zone icon that contains information on the volume of space used for calculation. “A

zone is a volumes of air separated from other volumes of air by walls, floor and ceiling.” [5] The duct systems that pressurized the stairwells were also developed.

3.3 Duct Layout

CONTAM modeling of the duct systems consisted of four supply fans, 20 supply terminals and four inlet terminals. On the ground floor and the 29th floor, each had two fans indicated by two asterisks (**) next to an airflow triangle (▲). There also were four inlet terminals located outside the building, which allowed for outside air to be supplied to the duct system. The inlet terminals and fans are shown in Figure 3 and Figure 4.

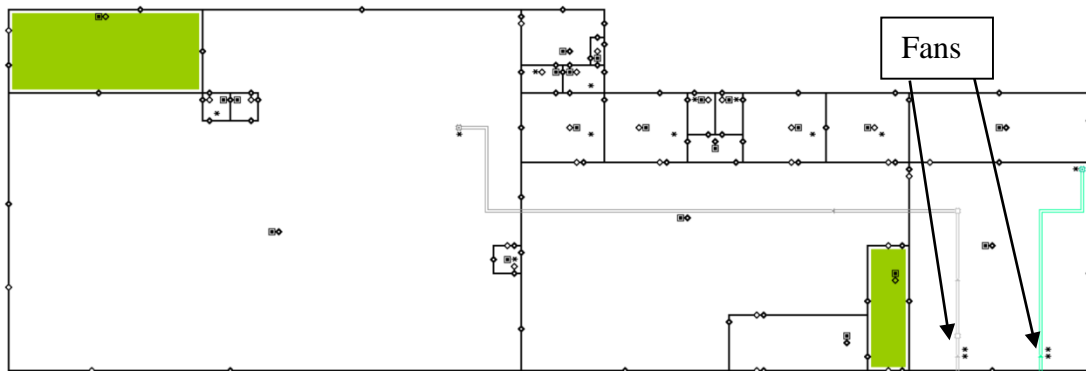


Figure 3: CONTAM model of the ground floor

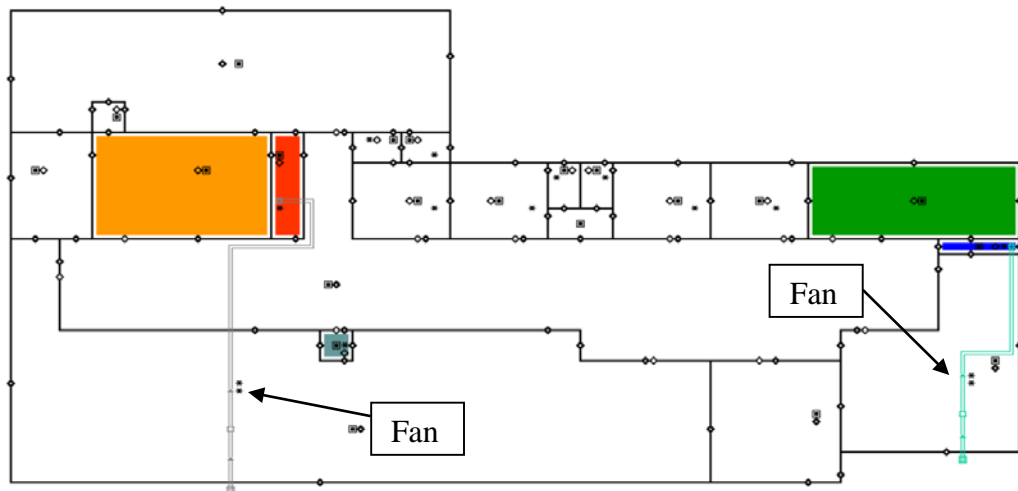


Figure 4: CONTAM model of the 29th floor.

As seen in Figures 2 and 3, the gray duct system supplied air to Stairwell_A and the green duct system supplied air to Stairwell_B. Each stairwell was accompanied by an adjacent duct shaft, Shaft_A for Stairwell_A and Shaft B for Stairwell_B. The gray supply fan on the ground floor supplied air to rectangular duct segments. Figure 5 shows that the duct traveled up through Shaft_A. This duct decreased in size with lower flow requirements as the duct approached the center of the building and the end of that duct run. At the 2nd, 4th, 7th, 10th, and 13th floors, the gray vertical duct feeds five terminals that disperse air into the stairwell. As shown in Figures 2 and 3, the gray supply fan on the 29th floor supplied air to rectangular duct segments. This duct traveled down through Shaft_A and similarly decreased in size with lower flow requirements as the duct approached the center of the building, as depicted in Figure 4. The gray vertical duct feeds five terminals that disperse air into the stairwell at the 16th, 19th, 22nd, 25th, and 28th floors. The green supply fan on the ground floor supplied air to rectangular duct segments that travel up through Shaft_B. The green vertical duct system and terminals dispersed air in the same manner as the gray vertical duct system. An isometric view of each stairwell with its adjacent duct shaft is illustrated in Figure 5 and Figure 6.

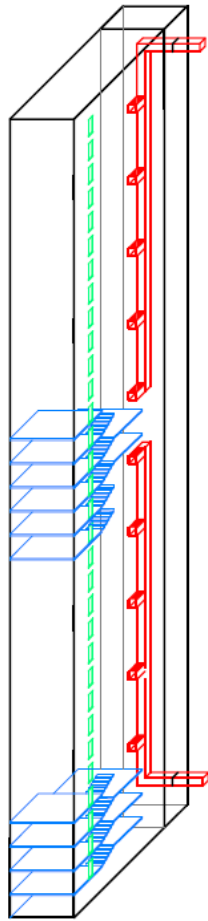


Figure 5: Isometric of Stairwell A and Shaft A with duct segments.

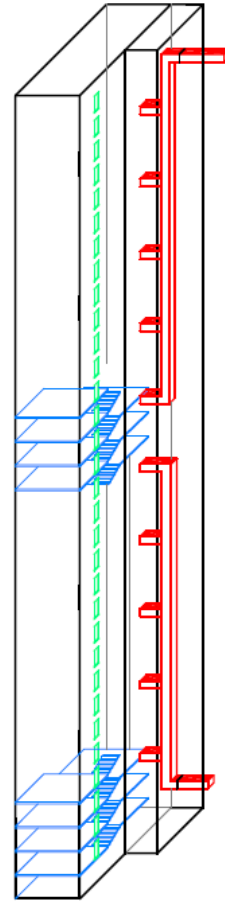


Figure 6: Isometric of Stairwell B and Shaft B with duct segments.

The isometric views show the location of each stairwell and duct shaft. Figure 5 represents an isometric view of Stairwell_A and Shaft_A with 10 supply air terminals. Similarly, Figure 6 represents an isometric view of Stairwell_B and Shaft_B with 10 supply air terminals. This building does not have a system for preventing over pressurization.

Chapter 4: CONTAM Inputs

Global inputs and changeable variables are two types of parameters used to create the multiple CONTAM models, which were used to examine the effects of duct leakage rates on fan capacity for stairwell pressurization. Global inputs stayed constant throughout each simulation. Changeable variables were used to examine the affects that variables had on each simulation. These two types of parameters produced 48 variations to the residential high-rise building model.

4.1 Global Inputs

The 48 simulations had global inputs that stayed constant throughout each simulation for consistency of the model and reduction of model variations. Global inputs consisted of ducts, flow paths, doors, zones and density.

4.1.1 Ducts System

The mechanical plans provided the rectangular duct layouts, sizes, the duct leakage material, and duct segment length. This information was added into the CONTAM models and stayed constant throughout each simulation.

The roughness factor was used in the airflow calculation for each duct segment. Galvanized steel duct is considered to have an average roughness category and an absolute roughness factor of 0.15 mm [6]. CONTAM has a default value of 0.09 mm, which is 40% percent less than ASHRAE recommended value. There are four other duct roughness factors that are suggested in the user guide for CONTAM:

- smooth at 0.03 mm,
- medium at smooth 0.09 mm,
- medium rough at 0.90 mm, and
- rough at 3.00 mm.

The ASHRAE value was used during all simulations. Keeping the roughness factor constant allowed for the leakage flow of the duct systems to be analyzed independently.

The duct sizes and floor level locations for all 48 simulations are illustrated in Figure 7. The vertical duct segments that traveled through the mechanical shaft stayed the same for both Shaft_A and Shaft_B. From the fan to the final discharge terminal, the duct sizes reduced as the flow requirements reduced. The following duct segment sizes were utilized from the fan to the final discharge terminal:

- 965 mm x 508 mm from the fan discharge,
- 762 mm x 508 mm,
- 609 mm x 457 mm, and
- 508 mm x 304 mm final discharge terminal.

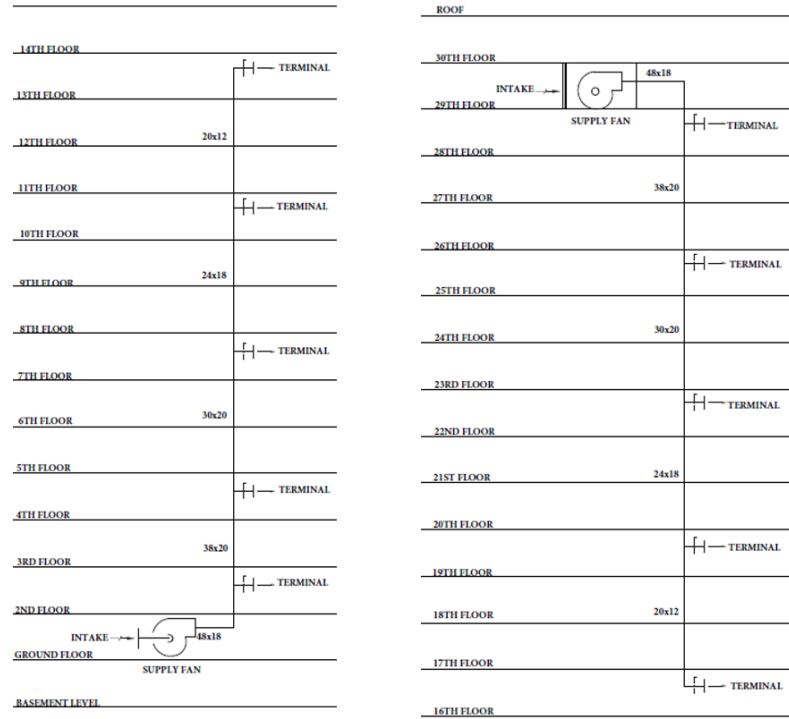


Figure 7: Duct sizes and fan location from Basement level to Roof used in the CONTAM models.

Junctions were placed at relative elevations (mid-height of the current level) and temperatures were adjusted during simulations to assess how the duct flow influenced and reacted to the building (stack effect or reverse stack effect). Terminal locations and relative elevations stayed constant throughout each simulation, while junction temperature was changed for each simulation to match the temperature of outside conditions.

Airflow entered or exited a duct through terminals which are the endpoints or starting points of a duct segment. The model showed four terminals located outside the building for pulled in outside air and ten terminals for supplied

outside air into each stairwell. The outside air was not heated or cooled in the duct system.

Parameters to determine how the duct flow influenced and reacted to stack effect in the stairwell were determined as follows:

- azimuth angle (direction terminal faces),
- balance loss coefficient (calculated for duct balance method then used value for steady state method – CONTAM default is zero),
- design flow rate (constant for duct balance method and dependent of fan capacity for steady state method),
- free face area (0.0314 m²),
- relative elevation (mid-height of the current level),
- temperature (-20°C, 20°C, and 40°C),
- terminal loss coefficient (0.125), and
- wind speed modifier (not applicable).

4.1.2 Airflow Paths Types

In CONTAM, an airflow component allowed air to move between two adjacent zones. Airflow components described vertical and horizontal air movement and pressure difference that occurred through stairwells, shafts, floor cracks, wall cracks and door openings. Each airflow path was provided with specific information to describe its flow characteristics by inputting information into an airflow element. Each airflow element used a one way-flow model that permits

flow in the direction of the lower pressure. The following power law models for the airflow elements were used: *Leakage Area Data Model* for doors, walls and floors; *Stairwell Model* for stairwells; and *Shaft Model* for shafts. The difference between these models is how the airflow movement is calculated. *Stairwell Model* relates airflow calculations to fit experimental data, while *Shaft Model* calculates airflow by using Darcy-Weisbach relation and Colebrook's equation for friction factor.

These mathematical models provided a relationship between air movement and pressure difference across each airflow path. The direction of flow between two zones was a function of the pressure drop along a path multiplied by a constant or the pressure differential as show in Equation 11 [5].

$$F_{ji} = f(P_j - P_i) \quad \text{Equation 11}$$

Where:

F_{ji} = airflow from zone j to zone i, kg/s

f = constant,

P_j = pressure at j=1, Pa

P_i = pressure at i=2, Pa

The pressure from zone 2 was subtracted from the pressure from zone 1. If the pressure differential was negative then the air moved into zone 1 from zone 2 and if the flow was positive then the airflow moved from zone 1 into zone 2. The flow paths that the air moved through for walls and door were placed at the

mid elevation of each floor level, while the airflow paths for floor, stairwell and shaft were placed at the floor elevation.

4.1.3 Doors

There were four different door types with leakage areas that remained constant throughout the 48 CONTAM models. These door with leakage areas are:

- Double exterior/interior doors having a leakage rate of 0.060 m^2 ,
- Single exterior/interior/bathroom doors having a leakage rate of 0.022 m^2 ,
- Single stairway doors having a leakage rate of 0.030 m^2 ,
- Elevator and linen doors having a leakage rate of 0.022 m^2 .

4.1.4 Zones

Each room shown in the CONTAM model is called a zone and required floor area input data. The floor area data was obtained from the mechanical plans and entered into the CONTAM model. Each zone temperature was uniform and pressure varied hydrostatically. The default temperature in CONTAM was 20°C and the pressure for each zone depended on the airflow passing through any orifice. For summer and winter weather conditions, the duct system supplied outside air into the stairwell and leaked into the mechanical shaft that caused a temperature difference. Which affected the airflow between the stairwell, mechanical shaft and the rest of the building.

4.1.5 Density

Parameters that relate to the treatment of air density can be changed in each simulations as follows:

- *Run steady state initialization to convergence,*
- *Adjust temperature in flow elements,*
- *Use of advanced hydrostatic equations,*
- *Vary density during time step.*

These parameters allowed for variations of zone air densities that provide a transient analysis opposed to the default quasi-steady analysis. The model defaults to quasi-steady model only when the *run steady state initialization to convergence* simulation was utilized. For this research, all air density parameters were activated to improve the airflow analyses. Each density parameter was described below.

Run steady state initialization to convergence parameter ran at the beginning of the simulation until the zone airflow, pressures, and densities converged. This allowed the airflow calculation to take into consideration changes in zone density due to pressurization or depressurization.

The *adjust temperature in flow elements* parameter took into account the actual air properties moving through each airflow element. This modified each airflow element coefficient. As a result, the computed flow changed by only a few percent.

The *vary density during time step* parameter allowed the zone density to vary within the Bernoulli's Equation 12 [5] shown below for each time step.

$$\Delta P = \left(P_1 + \frac{\rho V_1^2}{2} \right) - \left(P_2 + \frac{\rho V_2^2}{2} \right) + \rho g(z_1 - z_2) \quad \text{Equation 12}$$

Where:

ΔP = total pressure drop between zone 1 and zone 2, Pa

P_1 = static pressure at zone 1, Pa

P_2 = static pressure at zone 2, Pa

ρ = air density, kg/m³

V_1 = velocity at zone 1, m/s²

V_2 = velocity at zone 2, m/s²

g = acceleration of gravity (9.81 m/s²)

z_1 = elevation at zone 1, m

z_2 = elevation at zone 2, m

This simulation was completed when the airflow rates, densities and pressure converged. The maximum number of iterations required to complete the convergence was set at 100 compared to the model's default number of 20. This ensured airflow rate, density and pressure converge for each time step.

The CONTAM user manual described the *use of advanced hydrostatic equations*: "Typically the stack calculation is based on the incompressible

hydrostatic equation of the form $P_s = -\rho gh$. The advanced equation accounts for the change in density with the local zone reference pressure as well, and has the form $P_s = P_{ref}(e^{-gh/RT} - 1)$. These values are calculated for the inlet and outlets of each airflow path (and duct segment), and the difference is used to determine the contribution of the stack pressure to the overall pressure difference across the flow paths.” [5]

These four air density parameters allowed for an advanced analysis of air movement in a high-rise residential building by allowing each airflow, zone density and pressure to vary in Equation 13 [5]:

$$\frac{dm_i}{dt} = \rho_i \frac{dV_i}{dt} + V_i \frac{d\rho_i}{dt} = \sum_j F_{ji} + F_i \quad \text{Equation 13}$$

where:

$$\frac{dm_i}{dt} = \text{mass change per time of air in zone } i$$

$$\rho_i = \text{density at zone } i, \text{ where } i = 1,2$$

$$\frac{d\rho_i}{dt} = \text{density change per time}$$

$$V_i = \text{volume at zone } i, \text{ where } i = 1,2$$

$$\frac{dV_i}{dt} = \text{volume change per time}$$

$$F_i = \text{airflow rate from zone } i, \text{ kg/s (non-flow processes)}$$

When the density parameters are not varied during the analysis the flows are evaluated by assuming quasi-steady conditions to form Equation 14 [5]:

$$\sum_j F_{ji} = 0$$

Equation 14

4.2 Changeable Variables

Changeable variables consider 48 versions of the residential high-rise building by varying duct leakage rates, building leakages, outside temperatures and model simulation methods. Each variation of the building started with a duct leakage rate, which was then split into either a tight building leakage or loose building leakage. Then, each building leakage was split into three outside temperatures models. Each temperature model was then simulated with a duct balance simulation and a steady state simulation. One variation of the model breakdown is illustrated in Figure 8.

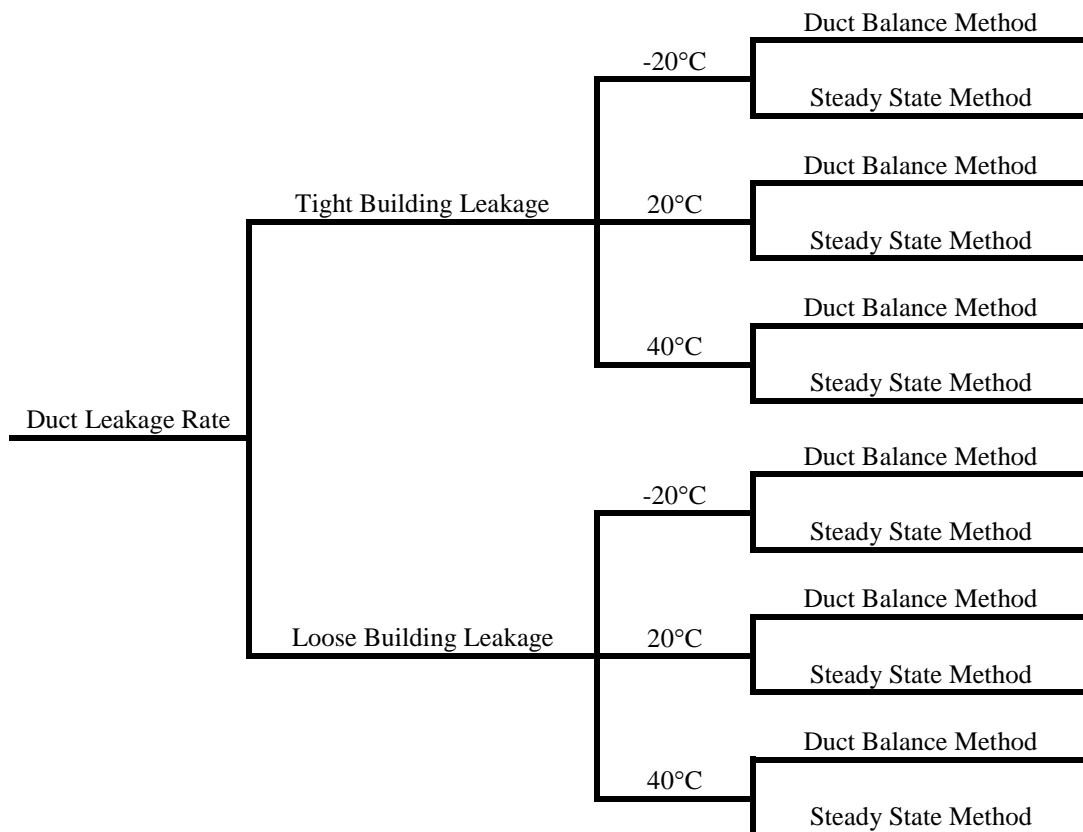


Figure 8: One variation of model simulation that produces 12 models

4.2.1 Duct Leakage Rates

Out of the 48 simulations, each set of 12 models had a different duct leakage rate for a total of four different duct leakage rates. The four different duct leakage rates and duct leakage classifications considered for the analyses are:

- Two sealed rates at 0.14 L/s/m² (4), and 0.62 L/s/m² (17),
- Two unsealed rates at 2.48 L/s/m² (68), and 5.6 L/s/m² (155) [6].

By substituting the leakage rate at a pressure difference of 250 Pa from ASHRAE, CONTAM calculated these leakage classifications:

- 0.14 L/s/m² gives a 3.9 classification,
- 0.62 L/s/m² gives a 17.2 classification,
- 2.48 L/s/m² gives a 68.7 classification, and
- 5.6 L/s/m² gives a 155.2 classification.

The CONTAM model provided a slightly greater classification for three of the leakage rates and one lesser compared to the classifications from ASHRAE Handbook – Fundamentals [6]. The CONTAM default leakage rate and leakage class is 0 L/s/m² (0) at a pressure difference of 1 Pa. The percent differences between ASHRAE and CONTAM for the four leakage rates were 2.5%, 1.2%, 1.0% and 0.1%, respectively.

4.2.2 Building Components

The building leakage properties for the 48 CONTAM models of which 24 variations of the models had a tight building leakage and other 24 variations of the models had a loose building leakage. There were four different types of

leakage elements; exterior building walls, stairwell walls, elevator shaft walls, and floors. Each had a different leakage for tight and loose leakage that were constant for each model. Categories of leakage area per unit wall area for tight leakage and loose building leakages are shown in Table 2 [2]:

Table 2: Building leakage rates for tight and loose leakage

	Leakage Area	
	Tight	Loose
Exterior building walls	$5.0 \times 10^{-5} \text{ m}^2/\text{m}^2$	$3.5 \times 10^{-4} \text{ m}^2/\text{m}^2$
Stairwell walls	$1.4 \times 10^{-5} \text{ m}^2/\text{m}^2$	$3.5 \times 10^{-4} \text{ m}^2/\text{m}^2$
Elevator shaft walls	$1.8 \times 10^{-4} \text{ m}^2/\text{m}^2$	$1.8 \times 10^{-3} \text{ m}^2/\text{m}^2$
Floors	$6.6 \times 10^{-6} \text{ m}^2/\text{m}^2$	$1.7 \times 10^{-4} \text{ m}^2/\text{m}^2$

The leakage area is the length of each wall segment multiplied by the floor height which is then used for the airflow path properties for the Power Law Model: *Leakage Area* routine in CONTAM to calculate the airflow and pressure change on each leakage surface. This model uses a modified version of the orifice equation (Equation 15) [5] for air infiltration. The modified version is used with leakage area formulation to calculate airflow.

$$L = \frac{Q_r \sqrt{\rho / 2 \Delta P_r}}{C_d}$$

Equation 15

Where:

L = effective leakage area, m^2

Q_r = predicted airflow rate at ΔP_r , m^3/s

ρ = density, kg/m^3

ΔP_r = reference pressure difference, 10 Pa

C_d = discharge coefficient of 0.6

4.2.3 Weather

This research considered three different weather conditions to study how temperature influences the building pressure and airflow movement. The three weather conditions considered were winter, summer and ambient (standard condition). The building temperature was maintained at a constant 20°C (standard condition) throughout the simulation. Sixteen model simulations included winter condition that had an outside temperature of -20°C. Sixteen model simulation considered summer conditions that had an outside temperature of 40°C. The last sixteen model simulations considered ambient conditions that have an outside temperature of 20°C (standard condition). When the outside temperature and building temperature were the same, the temperature was no longer a consideration on the airflow leaking out of each duct segment.

CONTAM used the air temperature to calculate the air density that passed through openings, door cracks, orifices, and wall leakage at each airflow point. Stairwell zones were considered to be maintained at the outside temperature due to the duct supplying outside air temperature into the stairwell based on an assumption that the transitions between initial indoor ambient conditions to outside temperature occurs quickly.

Three different outside temperatures at -20°C, 20°C, and 40°C were used for each duct leakage rate. The model duct system that pressurized each stairwell was designed not to heat or cool down the outside air that runs through the duct system. Each duct segment, terminal and junction temperature input data was assumed to match each outside temperature condition.

4.2.3 Simulation Methods

To determine the effects of duct leakage rates on fan capacity requirements without air contaminant, the following airflow simulation methods were used:

- Steady state, and
- Duct balance methods.

The steady state simulation method obtained airflow and pressure differential under a constant building system and outside temperature condition. The duct balance simulation worked with detailed duct systems by adjusting duct terminal balance coefficients to meet the inputted airflow rates at each terminal. Both simulation methods depend on the density, non-linear equation solver and linear equation solver parameters.

Chapter 5: Calibration

Each model used a multiple-injection pressurization system to maintain a tenable environment to control and reduce the migration of smoke into each stairwell. This system supplied air and increased the pressure inside each stairwell. This caused a pressure difference between the stairwell and the building.

For buildings without sprinkler systems, the minimal design pressure difference across a smoke barrier (door) is 0.10 inches of H₂O and shall be maintained under conditions of stack effect and wind. The minimal single door design pressure difference was met for each of the 24 simulations with the duct balance method and the 24 simulations with the steady state method. The multiple-injection pressurization system model was calibrated by modifying the airflow input parameter to the model until the output from the model provided a minimal door pressure difference for each stairwell.

5.1 Duct Balance Simulation Methods

Twenty four simulations used the duct balance method to assess the effect of duct leakage rates on fan capacity in the high-rise building model. The model was calibrated to meet the National Fire Protection Association standard requirement of a minimal door pressure difference of 0.10 in. H₂O [7]. This was done by adjusting the airflow out of the terminals. The model was calibrated to adjust for building leakage effect, duct leakage effect and stack effect.

This method used the terminal airflow and the loss coefficient to calculate the required fan capacity. The loss coefficient for the duct system changed for each simulation to account for airflow restrictions. Entering an airflow requirement for each terminal allowed the method to calculate a fan capacity to meet the airflow requirements at each terminal. All terminals that were located in each stairwell had the same airflow. Then the terminal airflows were adjusted to achieve the minimal door pressure difference. Every adjustment to the terminal airflow affected the building and stairwell pressure. These airflows were adjusted to compensate for this pressure change until the minimal door pressure difference was reached.

5.2 Steady State Simulation Methods

Twenty four of the models used the steady state simulation method to assess the effect of duct leakage rates on fan capacity. The model was calibrated to meet the National Fire Protection Association standard requirement of a minimal door pressure difference of 0.10 inches of H₂O [7]. This was accomplished by adjusting the airflow of each supply fan.

Airflow from the fan was sent to each terminal, to obtain pressure differentials under constant building temperature. The airflow out of each terminal is the amount of air supplied from the fan and distributed through the duct system from Darcy-Colebrook equations. Increasing or decreasing the entered fan capacity affected the air pressure created inside each stairwell. The fan capacity was adjusted until the minimal door pressure difference was reached for both stairwells. The model was calibrated to adjust for building leakages, duct leakages and stack effect.

5.3 Calibration Results

Each one of the 48 models was calibrated to meet a minimal door pressure difference of 0.01 inches of H₂O by either adjusting the airflow out of each terminal or by adjusting fan capacity, with consideration for building leakage effects, duct leakage effects and stack effects occurring in the high-rise building. Both the duct balance and steady state simulation methods showed that at least one doorway met the minimal pressure difference of 0.10 inches of H₂O as indicated in Table 3. The data for all doors pressure differences are presented in graphs in **Appendix B**.

Table 3: Shows the location of where the minimal door pressure difference of 0.10 inches of H₂O for each model.

Description	Temp.	Floor Number													
		31	30	29	28	27	26	25	24	23	22	21	20	~	6
SS-TB- DL1	-20°C		X*												
SS-TB- DL2	-20°C		X*												
SS-TB- DL3	-20°C		X*												
SS-TB- DL4	-20°C		X*												
SS-LB- DL1	-20°C		X*												
SS-LB- DL2	-20°C		X*												
SS-LB- DL3	-20°C		X*												
SS-LB- DL4	-20°C		X*												
SS-TB- DL1	20°C			X*			X*								
SS-TB- DL2	20°C		X*	X*			X*	X*	X*	X*	X*	X	X		
SS-TB- DL3	20°C		X*	X*		*	X*	X*	X*	X*	X*	X*			
SS-TB- DL4	20°C			X*			X*	X*	X*	X*					
SS-LB- DL1	20°C			X*		*	X*	*	*						
SS-LB- DL2	20°C			X*		X*	X*	*							
SS-LB- DL3	20°C			X*		X*	X*	*	*						
SS-LB- DL4	20°C			X*		X*	X*	X*	X						
SS-TB- DL1	40°C														X*
SS-TB- DL2	40°C														X*
SS-TB- DL3	40°C														X*
SS-TB- DL4	40°C														X*
SS-LB- DL1	40°C														X*
SS-LB- DL2	40°C														X*
SS-LB- DL3	40°C														X*
SS-LB- DL4	40°C														X*
		Floor Number													
		31	30	29	28	27	26	25	24	23	22	21	20	~	2
DB-TB- DL1	-20°C			X*			X*	X*	X*	X	X				
DB-TB- DL2	-20°C			*			X*	*	*	*					
DB-TB- DL3	-20°C						X*	*	*	*					
DB-TB- DL4	-20°C						X	X*	X*	*	*	*	*		
DB-LB- DL1	-20°C		X												*
DB-LB- DL2	-20°C		X												*
DB-LB- DL3	-20°C		X												*
DB-LB- DL4	-20°C		X												*
DB-TB- DL1	20°C		X*	X			X*	X	X	X	X	X	X		
DB-TB- DL2	20°C		X*	X		X	X*	X	X	X	X	X	X		
DB-TB- DL3	20°C		*	X*			X*	X*	X*	*					
DB-TB- DL4	20°C		X*	X*			X*	X*	X*	X*	X	X			
DB-LB- DL1	20°C			X*			X								
DB-LB- DL2	20°C			X*		X	X								
DB-LB- DL3	20°C			X*		X	X*								
DB-LB- DL4	20°C			X*		X	X	X	X						
DB-TB- DL1	40°C		X*												
DB-TB- DL2	40°C		X*												
DB-TB- DL3	40°C		X*												
DB-TB- DL4	40°C		X*												
DB-LB- DL1	40°C	X*													
DB-LB- DL2	40°C	X*													
DB-LB- DL3	40°C	X*													
DB-LB- DL4	40°C	X*													

* = represents where Stairwell_A minimal door pressure difference of 0.10 in.H₂O occurs

X = represents where Stairwell_B minimal door pressure difference of 0.10 in.H₂O occurs

SS - Steady state simulation method
DB – Duct balance simulation method

TB - Tight building leakage
LB – Loose building leakage

DL1 – Duct leakage rate 0.14 L/s/m²
DL2 – Duct leakage rate 0.62 L/s/m²
DL3 – Duct leakage rate 2.48 L/s/m²
DL4 – Duct leakage rate 5.6 L/s/m²

The steady state simulation method calculated a single set of airflows under a constant building system and weather conditions. At exterior temperatures of -20 and 40°C, the steady state methods for all building leakages, duct leakage classes and both stairwell locations met the minimal door pressure difference at the 30th and 6th floors. In contrast, for an exterior temperature of 20°C the minimal pressure difference occurred between the 31st and 20th floor. The duct balance method provided similar results in both stairwell locations for door pressure differences. The exception of this trend occurred for the case of an exterior temperature of -20°C and loose building leakage, the minimal door pressure difference occurred in Stairwell_A at the 2nd floor, while for Stairwell_B at the 30th floor.

Chapter 6: Data Analysis and Discussion

The data analysis examined the effects of temperatures, building components, and duct leakage rates on fan capacity requirement to pressurize both stairwells in a high-rise building. The effects of these changeable variables on the building pressure were studied. The fan capacity was examined for each stairwell and simulation method. Stairwell_A is located in the middle of the building surrounded by interior space, while Stairwell_B is located at a corner of the building with two walls exposed to outdoor conditions and two wall exposed to interior building conditions. The duct segments within the mechanical shaft which transport air to each stairwell were analyzed. The airflow that leaks out of the duct system affected the total fan capacity and building pressure. Each stairwell and the airflow occurring in each duct shaft was analyzed and discussed separately in this research.

6.1 Steady State Simulation Method – Stairwell_A and Shaft_A

The steady state method was used to run 24 CONTAM models previously discussed in section 5.2. The models considered the affects of temperature and building leakage for each duct leakage rate. This was done to evaluate the fan capacity required to pressurize Stairwell_A, which had two fans that supply air through the duct system located in Shaft_A. The two fan capacities were added and plotted against duct leakage rates for Stairwell_A. The duct leakage flow was plotted against floor level for Shaft_A.

The fan supplied air to a detailed duct system that were routed through mechanical Shaft_A and Shaft_B. The detailed duct system had four different leakage rates. The

leakage out of each junction point was collected for 24 models running a steady state simulation. The airflow leaking out of each junction point was plotted against floor level, to show how much air was leaking out for each temperature condition at each level.

The junction points started on the 3rd floor and went to the 30th floor, and there were no junction points on the 15th or 16th floors. The air flow data were collected for each temperature, while the building components varied from tight building leakage to loose building leakage. The data were grouped by temperature and airflow out of each duct junction point at each floor level.

6.1.1 Stairwell_A Data Analysis:

The fan capacity data for Stairwell_A showed a linear relationship between all four duct leakage rates when temperature and building components were constant. As illustrated in Figure 9, fan capacity increased as the temperature outside varied from the building temperature. For loose leakage, the data for winter, summer and standard temperature showed a change in fan capacity of 7.7%, 7.3% and 7.7%. These values were the total change in fan capacity when duct leakage rates increased from 0.14 to 5.6 L/s/m². The slopes between these duct leakage rates for each temperature condition were 0.57, 0.53 and 0.50 for loose building leakage. Tight leakage for summer, winter and standard temperature had slopes of 0.71, 0.60 and 0.52 with an increased change of 11.7%, 11.1% and 11% for fan capacity. All linear lines had a correlation coefficient of 0.99 and regressions ranging from 0.00292 to 0.10986, indicating that the points are

linearly related. With a high degree of confidence, there was a 95% chance each fan capacity point would lie near the linear line shown in Figure 9.

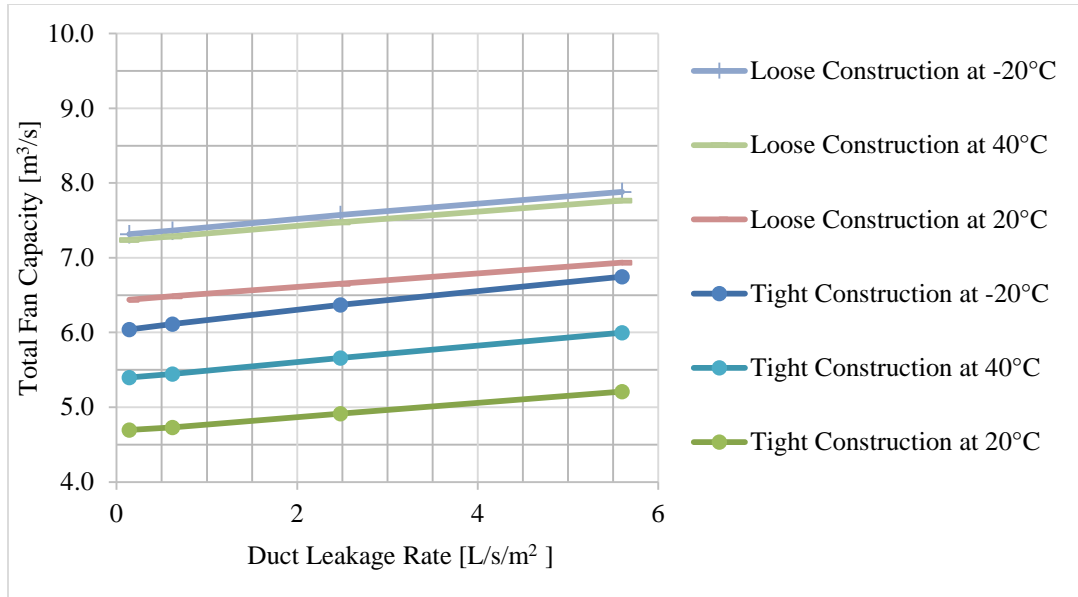


Figure 9: Duct leakage rate vs fan capacity for Stairwell_A running a steady state simulation for loose and tight building leakage.

As anticipated, the building leakage for loose leakage required a greater fan capacity than tight leakage shown in Figure 10.

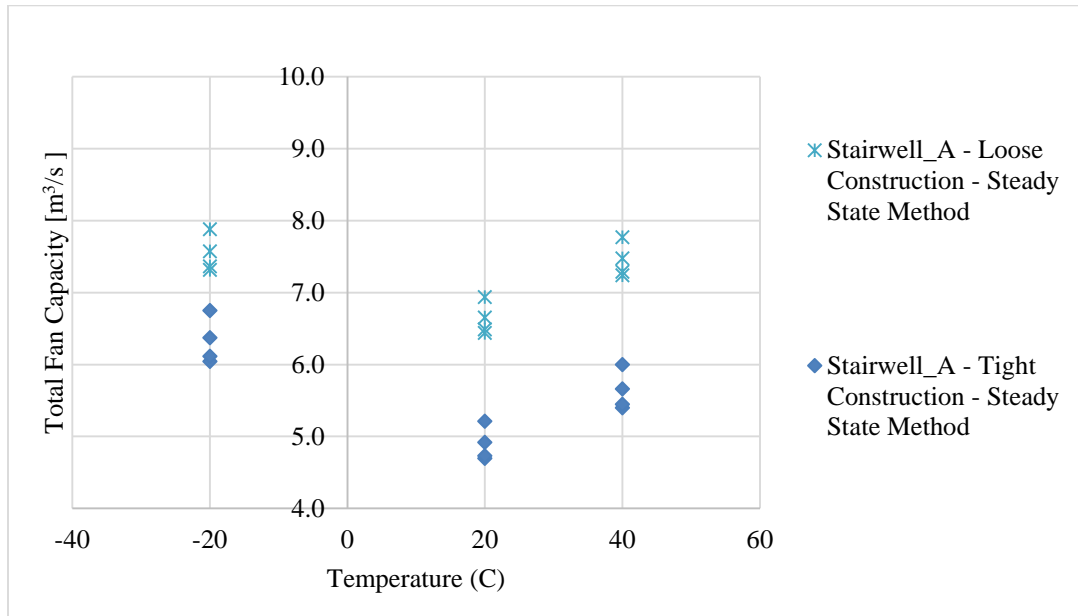


Figure 10: Outside weather conditions vs fan capacity for Stairwell_A. Running steady state method

6.1.2 Shaft_A Data Analysis:

The steady state simulation method for Shaft_A analyzed winter (-20°C), summer (40°C) and standard (20°C) exterior temperatures. Each temperature had eight different steady state simulations; four simulations with a tight building leakage and four with a loose building leakage. Each building component had four different duct leakage rates. The duct system decreased as it reached the center of the building from the top and bottom of the building. The air leaked out of each junction point decreased as it reached the center of the building. Each building leakage for each duct leakage rate runs parallel to one another. The data showed an increase in duct leakage at floors with open floor plans, which occurred on the 2nd, 6th, 28th and 29th floors. These open floor plans also affected the air leakage on the adjacent floors.

The duct airflow leaking out of each junction during winter conditions is shown in Figure 11 for both tight and loose leakage. The 3rd through 14th floors for a tight leakage showed a greater difference in air leakage than loose leakage. The 17th through 30th floors showed a lesser difference in air leakage for loose leakage than for tight leakage. The air leaking out of each duct segment was affected by the airflow pressurizing the stairwell. The loose building leakage allowed more airflow from the stairwell into the duct shaft, which reduced the airflow leaking out of the duct system. However, a tight building leakage reduced the airflow between the stairwell and the mechanical shaft allowing for an increase in air leakage out of the duct system.

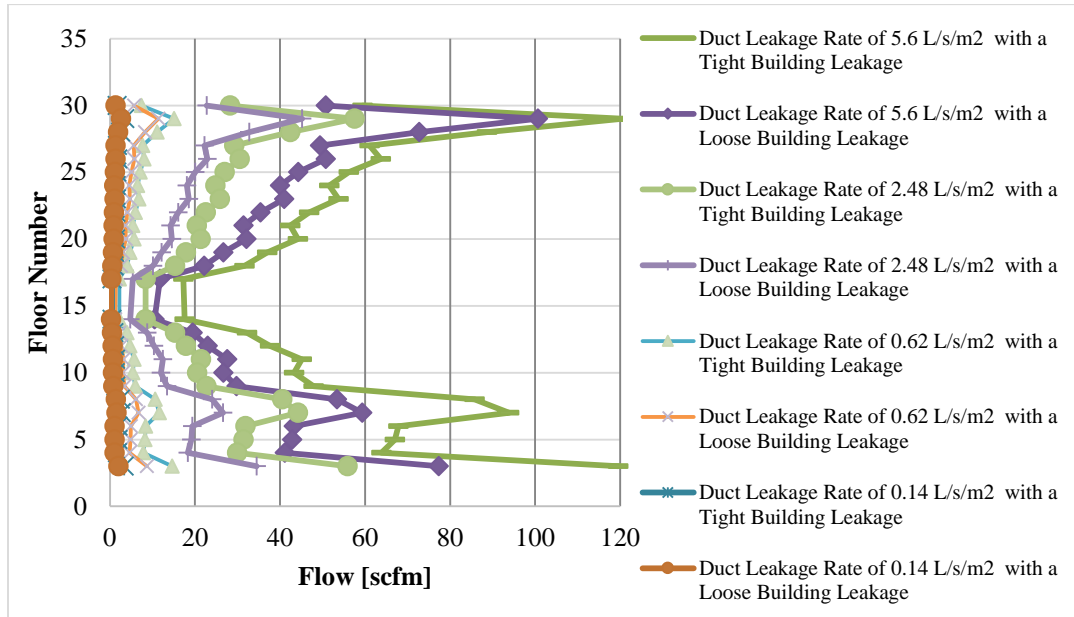


Figure 11: Airflow leakage from junction throughout Shaft_A during winter weather conditions for steady state simulation.

The duct airflow leaking out of each junction during summer conditions is shown in Figure 12 for both tight and loose leakage. The 3rd through 14th floors for a tight leakage showed a greater difference in air leakage than loose leakage, while the 7th through 30th floors had air leakages that were similar. The airflow between the stairwell and mechanical shaft had little effect on duct leakage between 17th through 30th floors. The summer conditions from 3rd to 14th floors were affected by the airflow leaking from the stairwell into the mechanical shaft. The loose building leakage showed a reduction in airflow leaking from the duct system compared to the tight building leakage for duct leakage rates of 2.48 and 5.6 L/s/m².

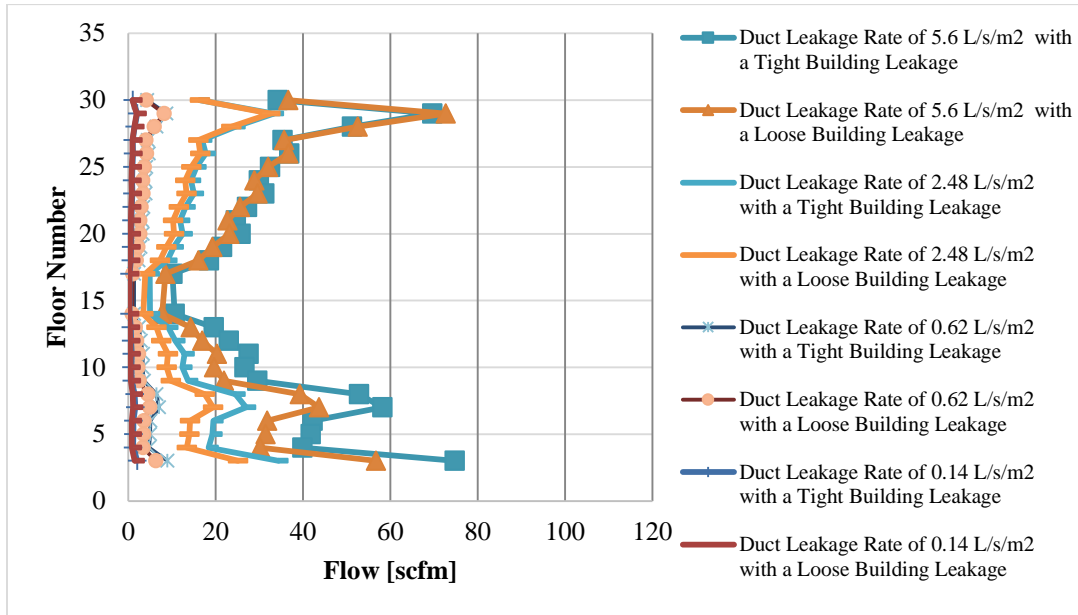


Figure 12: Airflow leakage from junction throughout Shaft_A during summer weather conditions for steady state simulation.

The duct airflow leaking out of each junction during standard temperature conditions is shown in Figure 13 for both tight and loose leakage. The data showed that both tight and loose leakage runs parallel to each other with the tight leakage having a slight increase in air leakage in the loose leakage. The airflow from the stairwell reduced the air leaking out of the duct system when the building components were loose, while having less of an effect on the duct leakage for a tight building leakage.

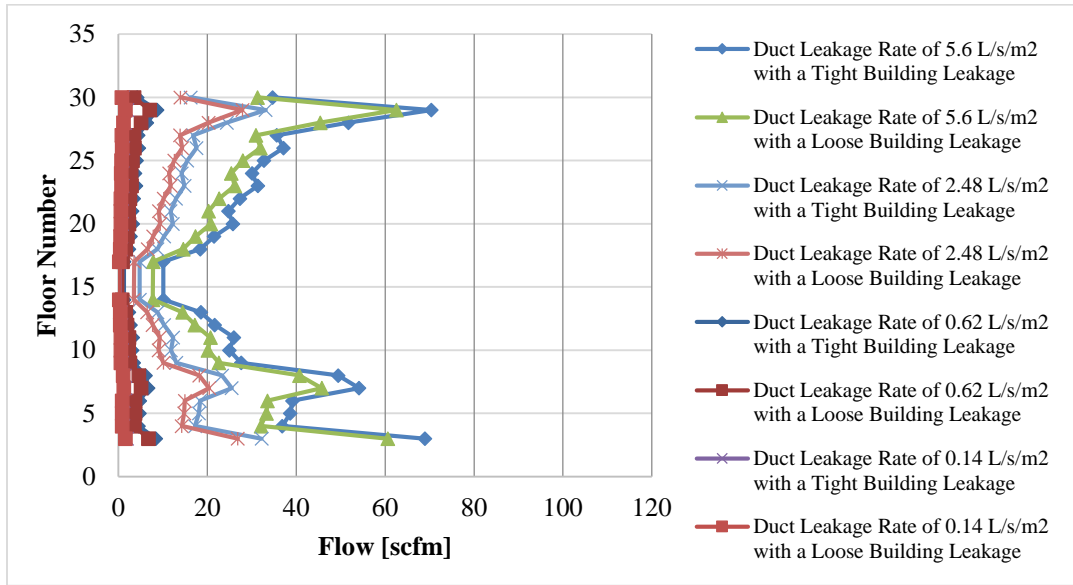


Figure 13: Airflow leakage from junction throughout Shaft_A during standard temperature for steady state simulation.

The data showed how sealed ducts produced less airflow leakage than unsealed ducts which caused the fan capacity to be reduced.

6.1.3 Summary:

Sealed ducts had a small percent change in fan capacity while unsealed ducts had an average change of 5% for both tight and loose building leakage. The difference between tight building leakages had roughly a 3% increase in total change of fan capacity than the loose building leakage. The difference in fan capacity from 20°C to either -20°C or 40°C is shown in Table 4. The steady state method for the tight building leakage resulted in a greater change in fan capacity from 20°C to -20°C than the loose building leakage.

Table 4: Summary of Stairwell_A fan capacity for steady state simulation

Description		Outside Temperature	Duct Leakage Rate	Total Fan Capacity	Percent Change in Sealed Duct	Percent Change in Unsealed Duct	Total Percent Change	Difference in Fan Capacity From 20C	Percent Change in Fan Capacity From 20C		
		°C	L/s/m ²	m ³ /s							
Tight Building Leakage	Steady State Simulation Method	Stairwell_A	-20	0.14	6.04	1%	11.7%	1.35	29%		
				0.62	6.11			1.38	29%		
				2.48	6.37	6%		1.46	30%		
				5.6	6.75			1.54	30%		
			20	0.14	4.69	1%	11.0%				
				0.62	4.73						
				2.48	4.92	6%					
				5.6	5.21						
		40	0.14	5.40	1%	11.1%	0.70	15%			
			0.62	5.45			0.72	15%			
			2.48	5.66	6%		0.74	15%			
			5.6	6.00			0.79	15%			
		Loose Building Leakage	Steady State Simulation Method	Stairwell_A	-20	0.14	7.3	1%	7.7%	0.88	14%
						0.62	7.4			0.88	14%
						2.48	7.6	4%		0.92	14%
						5.6	7.9			0.95	14%
20	0.14				6.4	1%	7.7%				
	0.62				6.5						
	2.48				6.7	4%					
	5.6				6.9						
40	0.14			7.24	1%	7.3%	0.80	12%			
	0.62			7.29			0.80	12%			
	2.48			7.48	4%		0.82	12%			
	5.6			7.77			0.83	12%			

6.2 Duct Balance Simulation Method – Stairwell_A and Shaft_A

6.2.1 Stairwell_A Data Analysis:

The fan capacity data for Stairwell_A, while running duct balance simulation method, increased linearly when duct leakage rate increased from 0.14 to 5.6 L/s/m², for each set of temperatures and building leakages. As illustrated in Figure 14, fan capacity increased as the temperature outside was different from the building temperature. Summer (40°C), winter (-40°C) and standard (20°C) exterior temperatures for loose leakage had a slope of 0.61, 0.35 and 0.48 with an increased change in fan capacity of 6.9%, 4.8% and 7.5%. These values were the total change in fan capacity when duct leakage rates increased from 0.14 to 5.6 L/s/m². Tight leakage for summer, winter and standard temperatures had a slope of 0.55, 0.42 and 0.51 with an increased change of 12%, 8.9% and 11%, respectively. There was very little difference in fan capacity for tight building leakage when exterior temperature changed. All the linear lines had a correlation coefficient of 0.99 and regressions ranging from 0.00626 to 0.10992, indicating that the points are linearly related. With a high degree of confidence, there was a 95% chance each fan capacity would lie near the linear line shown in Figure 14.

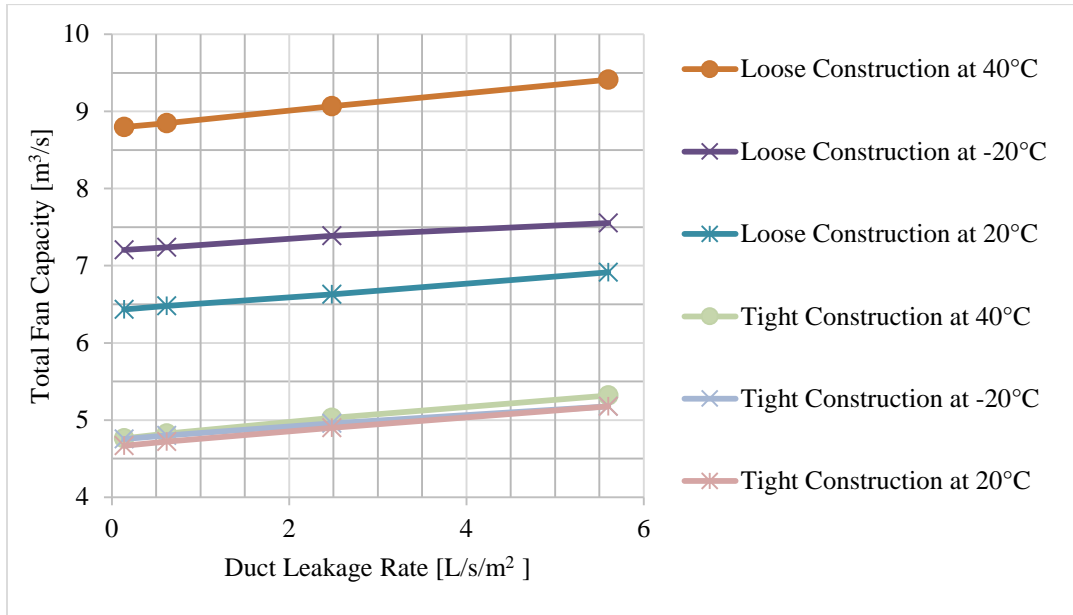


Figure 14: Duct leakage rate vs fan capacity for Stairwell_A running a duct balance simulation for loose and tight building leakage

The duct balance method showed a greater fan capacity difference for loose building leakage than tight building leakage as shown in Figure 15. Tight building leakage had fan capacities occurring around 5 m³/s, while loose building leakage had fan capacities ranges from 6.4 to 9.4 m³/s indicating a total increase of 46% in fan capacity.

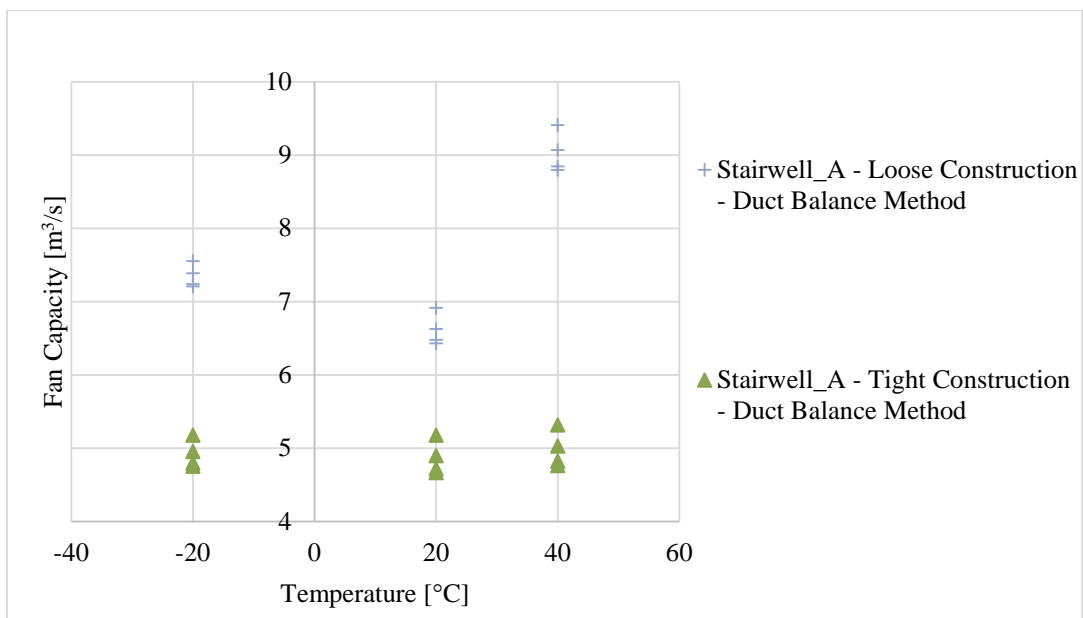


Figure 15: Outside weather conditions vs fan capacity for Stairwell_A. Running duct balance method

6.2.2 Shaft_A Data Analysis:

The duct balance simulation method for Shaft_A at summer (40 °C), winter (-40 °C) and standard (20 °C) exterior temperatures was analyzed. Each temperature had eight different duct balance simulations: four simulations with a tight building leakage and four with a loose building leakage. Each building component had four different duct leakage rates. The duct system decreased in size as it reached the center of the building from the top and bottom of the building. The air leaked out of each junction point decreased as it reached the center of the building. Each building component for each duct leakage rate ran parallel to one another. The data showed a large increase in duct leakage at floors with open floor plans, which occurred on the 2nd, 6th, 28th and 29th floors. These open floor plans affected the air leakage on the adjacent floors.

The duct airflow leaking out of each junction during summer temperature is shown in Figure 16 for both tight and loose leakages. Loose leakage had a slightly higher air leakage than tight leakage. This showed that summer exterior temperature does not affect the duct leakage rate for duct balance simulation. The airflow from the stairwell into the mechanical shaft was lower for a loose building leakage than for a tight building leakage. This lower airflow may cause an increase of air to leak out from duct systems, since the overall leakage was greater for the loose building than for the tight building leakages. However, pressure difference inside a tight building leakage was greater than in a loose building leakage.

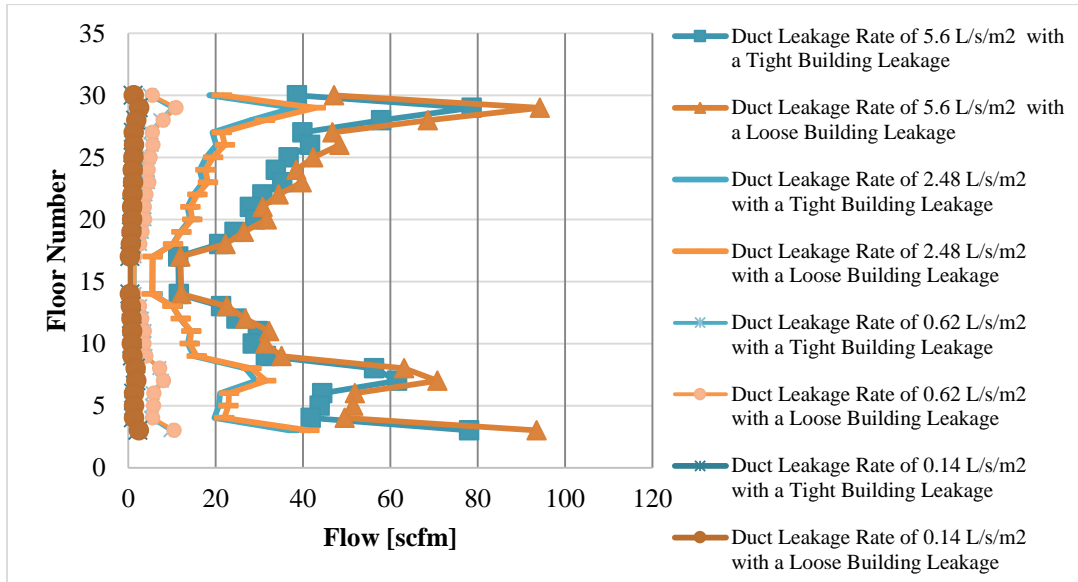


Figure 16: Airflow leakage from junction throughout Shaft_A during summer weather conditions for duct balance simulation.

The duct airflow leaking out of each junction during standard temperature is shown in Figure 17 for both tight and loose leakage. Loose leakage had a slightly lower air leakage than tight leakage. The duct leakage data showed loose leakage had less of an effect on fan capacity than tight leakage. The airflow from the stairwell was lower for the air leaking out of the duct system when the building leakage was loose, while having less of an effect on the duct leakage for a tight building leakage.

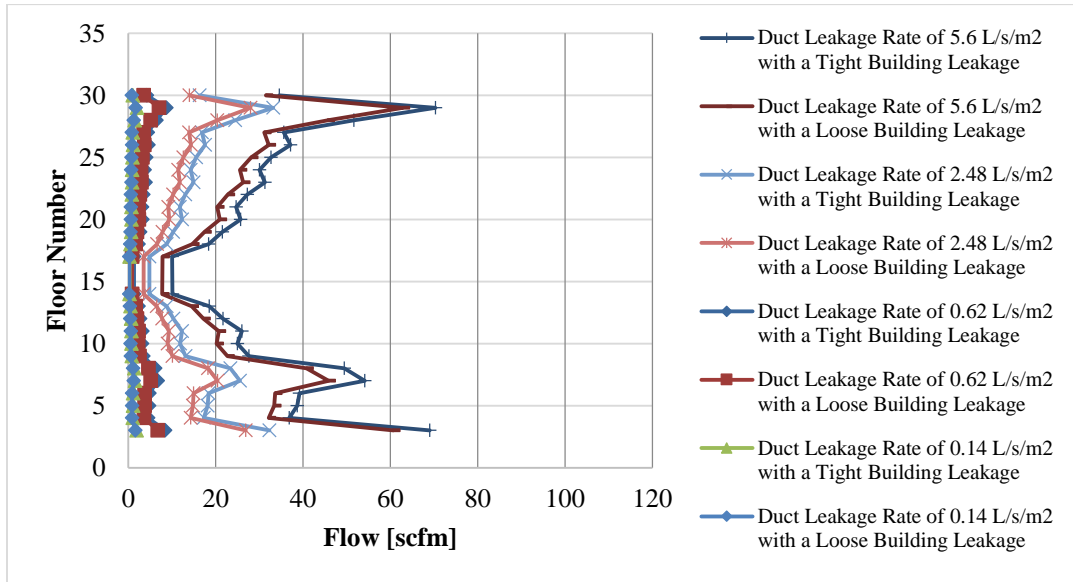


Figure 17: Airflow leakage from junction throughout Shaft_A during standard temperature (20°C) for duct balance simulation.

The duct airflow leaking out of each junction during winter temperature (-20°C) is illustrated in Figure 18 for both tight and loose leakage. Loose leakage had a slightly lower air leakage than tight leakage. The duct leakage data showed loose leakage had less of an impact on fan capacity than tight leakage. The loose building leakage was less effected by the duct leakage rates than the tight building leakage which may have been caused by an airflow leaking into the mechanical shaft from the stairwell.

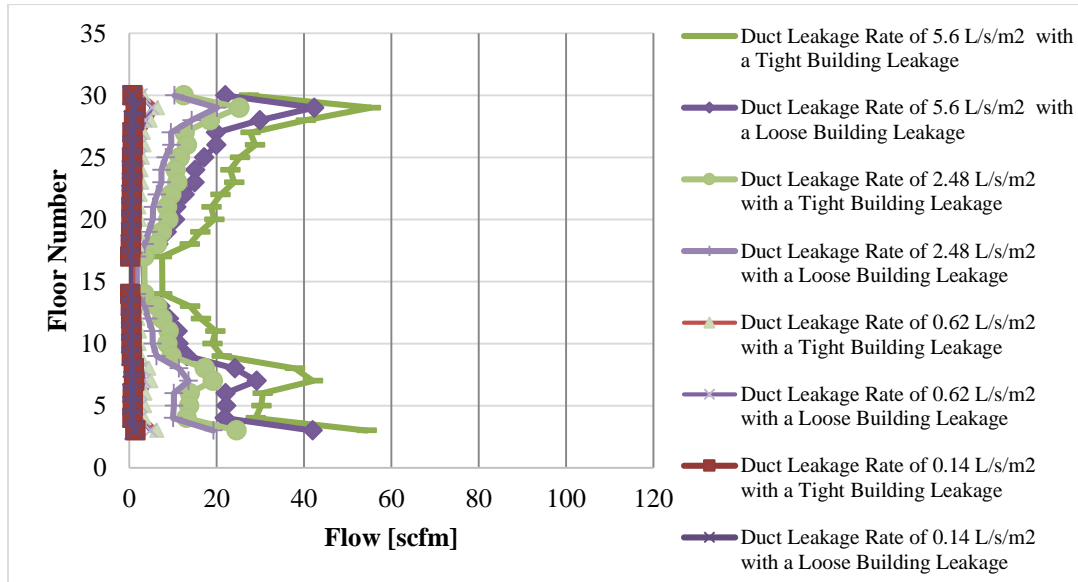


Figure 18: Airflow leakage from junction throughout Shaft_A during winter temperature (-20 °) for duct balance simulation.

The greatest airflow leakage out of the junctions occurred during summer temperature (40°C) followed by standard temperature (20°C) and then winter temperature (-20°C).

6.2.3 Summary:

Sealed ducts had a small percent change in fan capacity, while unsealed ducts had an average change of 5% for tight and 3% for loose building leakage. The difference between tight building leakages was roughly a 4% increase in total change of fan capacity than the loose building leakages. The difference in fan capacity from 20°C to either -20°C or 40°C is shown in Table 5. The duct balance method for a loose building leakage resulted in a greater change in fan capacity from 20°C. The tight building leakages had roughly the same fan capacity for all temperatures.

Table 5: Summary of Stairwell_A fan capacity for duct balance simulation

Description	Outside Temperature	Duct Leakage Rate	Total Fan Capacity	Percent Change in Sealed Duct	Percent Change in Unsealed Duct	Total Percent Change	Difference in Fan Capacity From 20C	Percent Change in Fan Capacity From 20C			
	°C	L/s/m ²	m ³ /s								
Tight Building Leakage	Duct Balance Simulation Method	Stairwell_A	-20	0.14	4.76	1%	8.9%	0.09	2%		
				0.62	4.80			0.08	2%		
				2.48	4.96	4%		0.06	1%		
				5.6	5.18			0.00	0%		
			20	0.14	4.67	1%	11.0%	6%			
				0.62	4.72						
				2.48	4.90						
				5.6	5.18						
			40	0.14	4.76	1%	11.7%	6%		0.10	2%
				0.62	4.82					0.10	2%
				2.48	5.03	0.13				3%	
				5.6	5.32	0.14				3%	
Loose Building Leakage	Duct Balance Simulation Method	Stairwell_A	-20	0.14	7.21	0.5%	4.8%	0.77	12%		
				0.62	7.24			0.76	12%		
				2.48	7.39	2%		0.76	11%		
				5.6	7.56			0.64	9%		
			20	0.14	6.43	1%	7.5%	4%			
				0.62	6.48						
				2.48	6.63						
				5.6	6.92						
			40	0.14	8.80	1%	6.9%	4%		2.37	37%
				0.62	8.85					2.37	37%
				2.48	9.07	2.44				37%	
				5.6	9.41	2.49				36%	

6.3 Steady State Simulation Method – Stairwell_B and Shaft_B

6.3.1 Stairwell_B Data Analysis:

The stairwell located in the corner of the building showed a linear increase of fan capacity for each set of building components and outside temperature. The steady state simulation results for Stairwell_B are shown in Figure 19. The greatest fan capacity occurred at -20°C for both tight and loose leakage. The fan capacity data for Stairwell_B showed a linear increase for loose leakage at -20, 40 and 20°C with a slope of 0.24, 0.29 and 0.23, respectively. The corresponding percent change increases in fan capacity at each duct leakage were 3.1%, 4.0% and 3.4% when the duct leakage rate increased from 0.14 to 5.6 L/s/m². The results for tight building leakage with the same temperatures had linear slopes of 0.26, 0.27 and 0.24. The fan capacity percent change increases for the tight wall were 4.6%, 5.3% and 5.6% when the duct leakage rate increased from 0.14 to 5.6 L/s/m². The fan capacities for the tight building leakage were slightly greater than for the loose building leakage.

All linear lines had a correlation coefficient of 0.99 and regressions ranging from 0.10076 to 0.10891, indicating that the points were linearly related. With a high degree of confidence, there was a 95% chance each fan capacity would lie near the linear line.

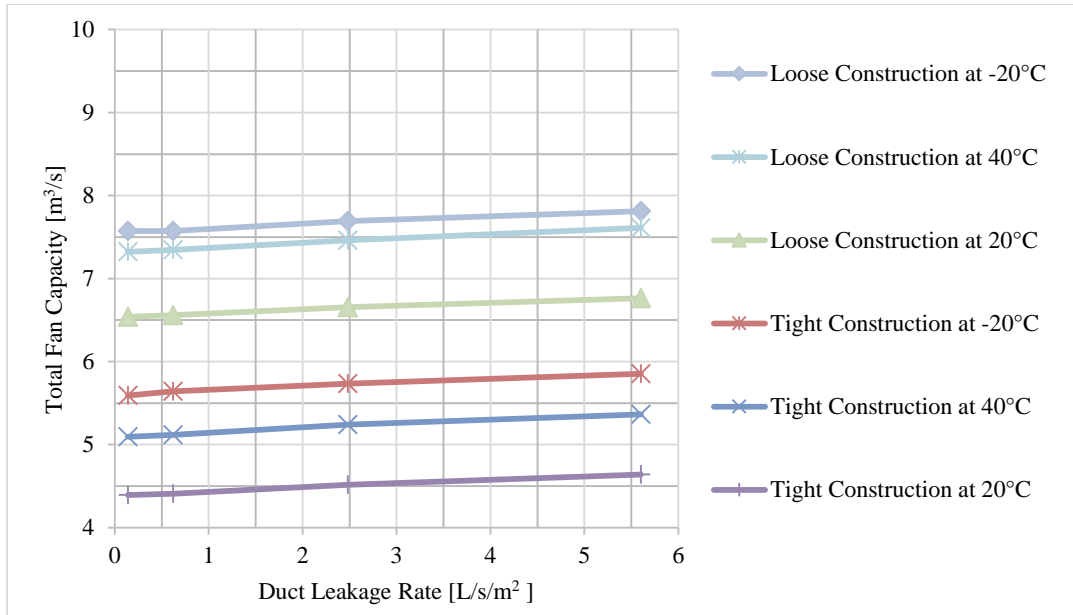


Figure 19: Duct leakage rate vs fan capacity for Stairwell_B running a steady state simulation for loose and tight building leakage.

The steady state method showed a greater fan capacity difference for loose leakage than tight leakage as indicated in Figure 20. The fan capacity for each duct leakage rate showed a tight grouping for all temperatures. The fan capacity data showed a similar increase in fan capacity from tight to loose leakage for each temperature.

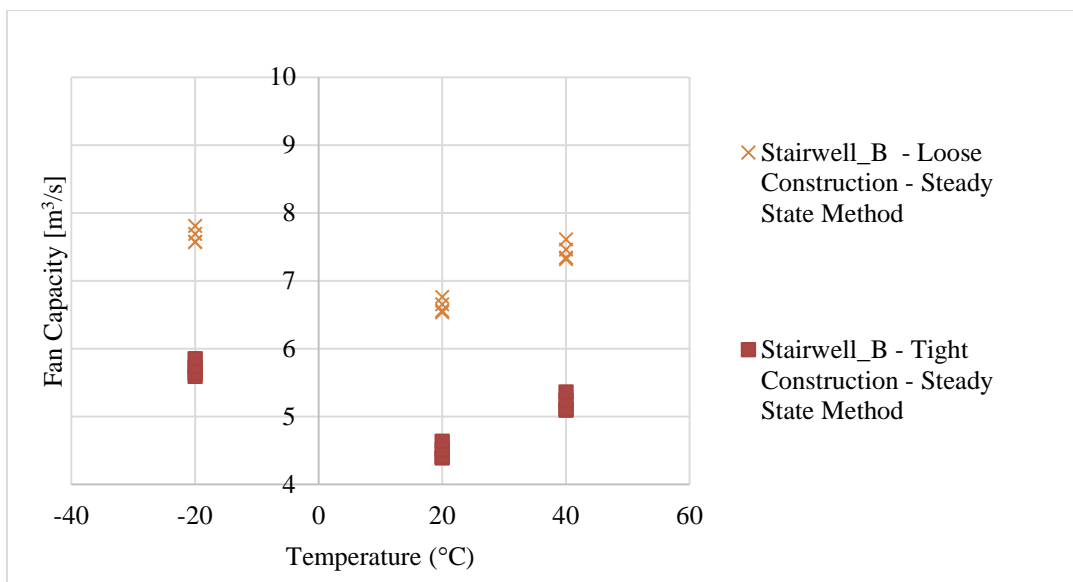


Figure 20: Outside weather conditions vs fan capacity for Stairwell_B. Running steady state method

6.3.2 Shaft_B Data Analysis:

The steady state method for Shaft_B at summer, standard and winter exterior temperatures was analyzed. Each temperature condition had eight different steady state simulations; four simulations with tight building leakage and four with a loose building leakage. Each building leakage had 4 different duct leakage rates. Similar to the other simulations, the duct system decreased as it reached the center of the building from the top and bottom of the building. The air leaked out of each junction point decreased as it reached the center of the building. Each building leakage for each duct leakage rate ran parallel to one another. The fan capacity data showed an increase in duct leakage when the building floor plan was open which occurs on the 2nd, 6th, 28th and 29th floors. These open floor plans affect the air leakage on the adjacent floors.

The duct airflow leaking out of each junction during winter temperature (-40°C) is shown in Figure 21 for both tight and loose leakage. Loose building leakage had a slightly higher air leakage than tight building leakage. The steady state simulations for tight and loose building leakages at winter temperatures provided similar results for duct leakages of 0.14 L/s/m², 0.62 L/s/m², 2.48 L/s/m², but duct leakage of 5.6 L/s/m² showed an increase in fan capacities. The airflow from the stairwell was much greater for a tight building leakages, which may have lowered the air leaking out of the duct system than for a loose building leakage.

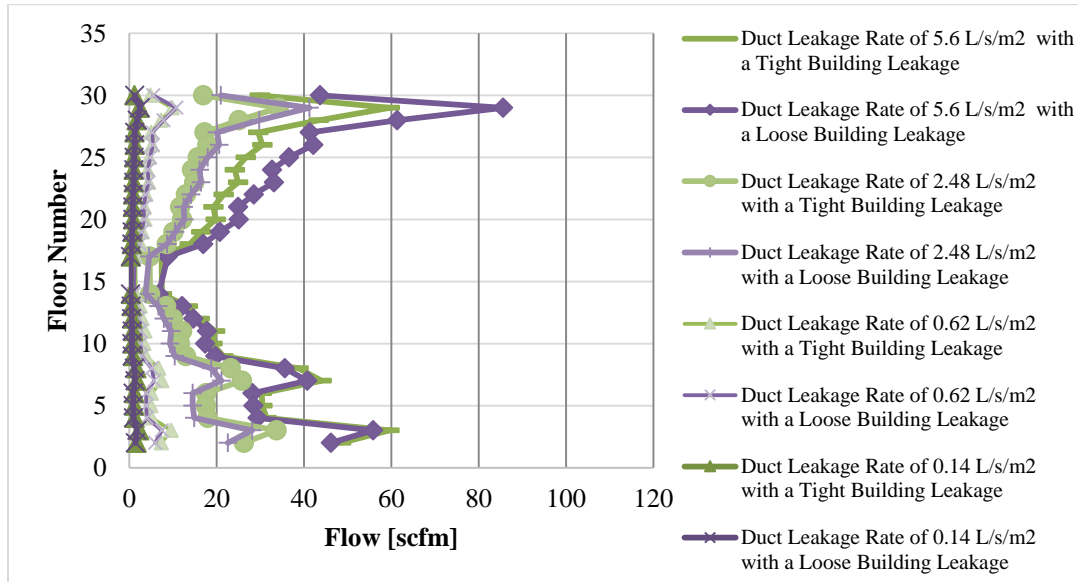


Figure 21: Airflow leakage from junction throughout Shaft_B during winter temperature (-20 °C) for steady state simulation.

The duct airflow leaking out of each junction during summer temperature (40°C) is shown in Figure 22 for both tight and loose building leakage. Loose building leakage had a slightly higher air leakage than a tight building leakage. Under the steady state simulation during summer temperature no differences were observed for the duct leakage rates of 0.14 L/s/m², 0.62 L/s/m², 2.48 L/s/m², 5.6 L/s/m² for both tight and loose building leakage, except for the duct leakage rate of 5.6 L/s/m² between the 17th and 30th floors. For both a tight and loose building leakages, the airflow was leaking from the stairwell into the mechanical shaft. However, the mechanical shaft leaked air into the hallway through the adjacent wall for the loose building leakage, while the reverse happened for a tight building leakage.

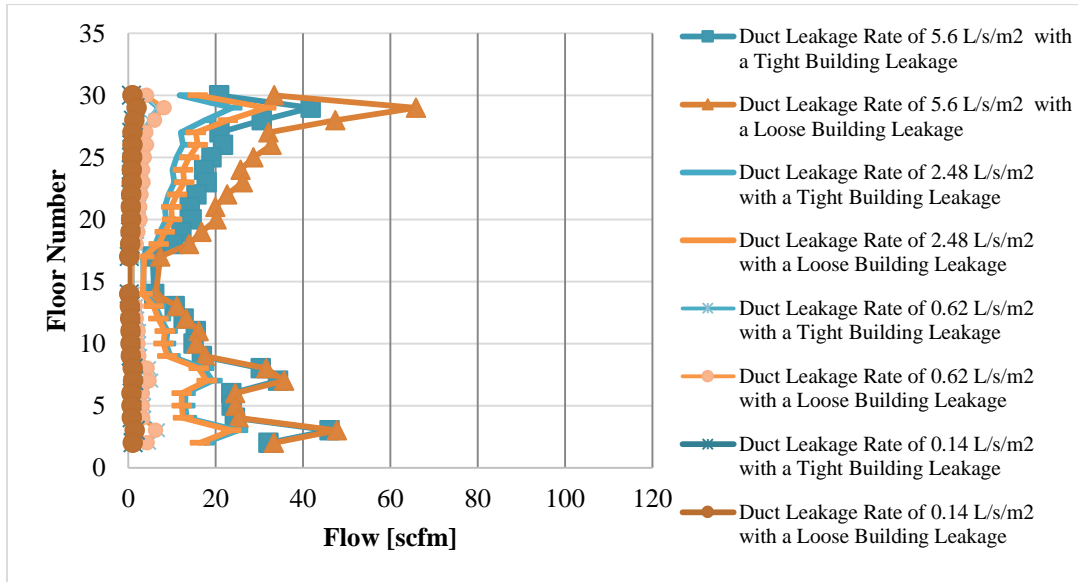


Figure 22: Airflow leakage from junction throughout Shaft_B during summer temperature (40°C) for steady state simulation.

The duct airflow leaking out of each junction during standard temperature (20°C) is shown in Figure 23 for both tight and loose leakage. As anticipated the loose leakage had a slightly higher air leakage than tight leakage. Under the steady state simulation method for standard temperature no differences were observed for the duct leakage rates of 0.14 L/s/m², 0.62 L/s/m², and 2.48 L/s/m² for tight and loose building leakages. As anticipated, the duct system with the highest leakage rate of 5.6 L/s/m², the fan capacities increased when the building leakage changed from tight to loose leakages at standard temperature. The airflow leaking from the stairwell and from the outside caused a higher duct leakage for a loose building over a tight building leakages.

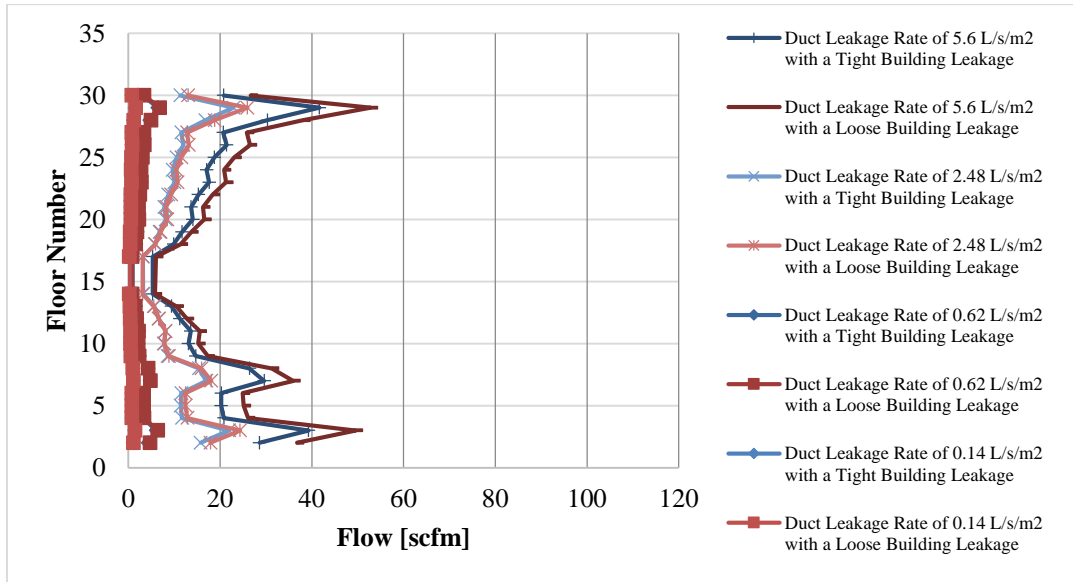


Figure 23: Airflow leakage from junction throughout Shaft_B during standard temperature (20 °C) for steady state simulation.

As the airflow leakage increased from tight and loose leakages, the required fan capacity to pressurize the system increased.

6.3.3 Summary:

Sealed ducts had a small percent change in fan capacity, while unsealed ducts had an average change of 2% for both tight and loose building leakages. The difference between tight building leakages was roughly a 2% increase in total change of fan capacity than the loose building leakage. The difference in fan capacity from 20°C to either -20°C or 40°C is shown in Table 6. The steady state method for tight building leakage resulted in a greater change in fan capacity from 20°C to -20°C than the loose building leakage.

Table 6: Summary of Stairwell_B fan capacity for steady state simulation

Description	Outside Temperature	Duct Leakage Rate	Total Fan Capacity	Percent Change in Sealed Duct	Percent Change in Unsealed Duct	Total Percent Change	Difference in Fan Capacity From 20C	Percent Change in Fan Capacity From 20C				
	°C	L/s/m ²	m ³ /s									
Tight Building Leakage	Steady State Simulation Method	Stairwell_B	-20	0.14	5.59	1%	4.6%	1.20	27%			
				0.62	5.64			1.23	28%			
				2.48	5.73	2%		1.22	27%			
				5.6	5.85			1.21	26%			
			20	0.14	4.39	0.3%	5.6%					
				0.62	4.41							
				2.48	4.52	3%						
				5.6	4.64							
			40	0.14	5.09	0.5%	5.3%	0.70	16%			
				0.62	5.12			0.71	16%			
				2.48	5.24	2%		0.72	16%			
				5.6	5.36			0.73	16%			
			Loose Building Leakage	Steady State Simulation Method	Stairwell_B	-20	0.14	7.57	0.0%	3.1%	1.04	16%
							0.62	7.57			1.01	15%
							2.48	7.69	2%		1.04	16%
							5.6	7.81			1.05	15%
20	0.14	6.54				0.3%	3.4%					
	0.62	6.56										
	2.48	6.66				2%						
	5.6	6.76										
40	0.14	7.32				0.3%	4.0%	0.78	12%			
	0.62	7.34						0.78	12%			
	2.48	7.46				2%		0.81	12%			
	5.6	7.61						0.85	13%			

6.4 Duct Balance Simulation Method - Stairwell_B and Shaft_B

6.4.1 Stairwell_B Data Analysis:

The duct balance simulation results for Stairwell_B are shown in Figure 24. The greatest fan capacity occurred linearly at 40°C (summer temperature) for loose building leakage. The data showed a linear increase for loose leakage during summer, winter, and standard temperatures having a slope of 0.24, 0.21 and 0.24. The fan capacity percent change increases for each temperature were 2.7% at 40°C, 2.7% at -20°C and 3.7% at 20°C when the duct leakage rates increased from 0.14 to 5.6 L/s/m². This showed a slight difference in each linear relationship between duct leakage rates.

For tight leakage the data showed a linear increase for winter, summer and standard temperatures having slopes of 0.22, 0.24, and 0.26, respectively. The fan capacity percent change increases were slightly higher than loose leakage of 4.8%, 5.5% and 5.9% when the duct leakage rates increased from 0.14 to 5.6 L/s/m². All linear lines had a correlation coefficient ranging from 0.98 to 0.99 and regressions ranging from 0.10627 to 0.02494, indicated that the points are linearly related. With a degree of confidence, there was a 95% chance each fan capacity would lie near the linear line.

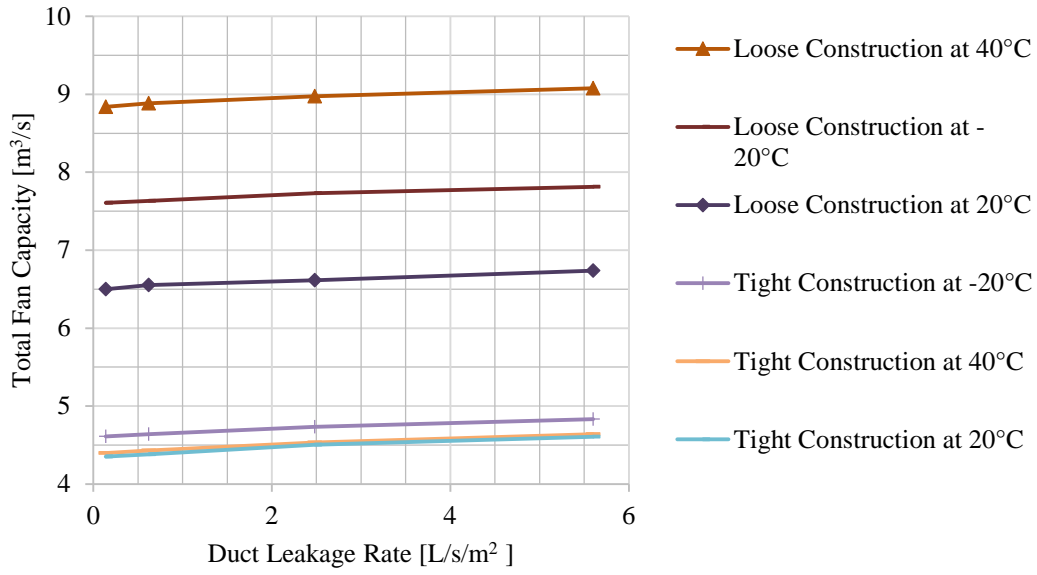


Figure 24: Duct leakage rate vs fan capacity for Stairwell_B running a duct balance simulation for loose and tight building leakage.

As illustrated in Figure 25, the duct balance method showed a greater fan capacity difference for the loose building leakages than for the tight building leakages. The tight leakages had a similar fan capacity for all temperatures, while the fan capacities for loose leakages varied for each temperature.

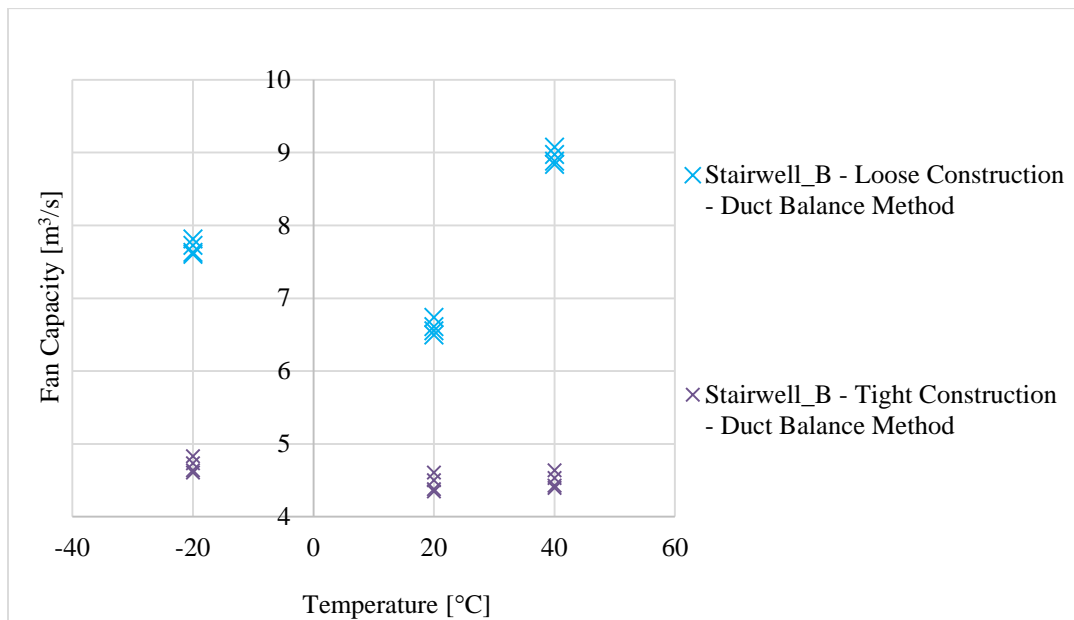


Figure 25: Outside weather conditions vs fan capacity for Stairwell_B. Running duct balance method

6.4.2 Shaft_B Data Analysis:

Summer, standard and winter temperatures were analyzed under the duct balance method for Shaft_B. Each temperature had eight different duct balance simulations: four simulations with tight building leakage and four with a loose building leakage. Each building leakage had four different duct leakage rates. The duct system decreased as it reached the center of the building from the top and bottom of the building. The air leaking out of each junction point decreased as it reached the center of the building. Each building leakage for each duct leakage rate is parallel to one another. The data showed an increase in duct leakage when the building floor plan was open, which occurred at the 2nd, 6th, 28th and 29th floors. These open floor plans affected the air leakage on the adjacent floors.

Figure 26 showed the duct airflow leaking out of each junction during summer conditions for both tight and loose leakage. The loose building leakages had a higher air leakage than for the tight building leakages. The duct balance simulation method for summer temperature affected the duct leakage rates of 0.14 L/s/m², 0.62 L/s/m², 2.48 L/s/m² and 5.6 L/s/m² for tight and loose leakages, which affects the amount of airflow supplied to the detailed duct system. The airflow leaking from the stairwell and from the outside increased the duct leakage for loose building leakages over tight building leakages.

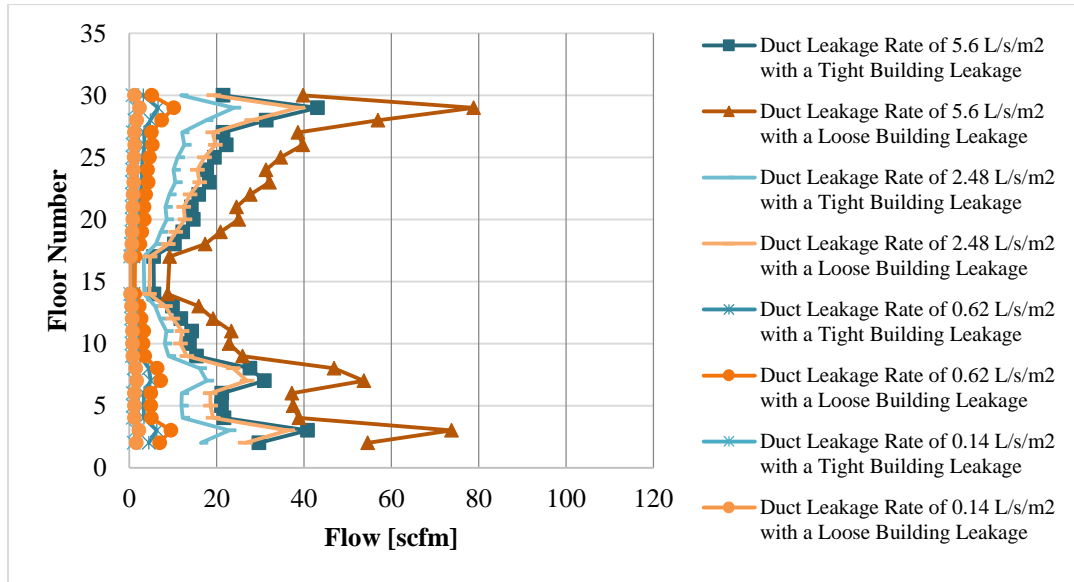


Figure 26; Airflow leakage from junction throughout Shaft_B during summer temperature conditions for duct balance simulation.

At standard temperature, the duct airflow leaking out of each junction is illustrated in Figure 27 for tight and loose building leakages. The loose building leakages had slightly higher air leakage than for the tight building leakages. The duct balance simulation method for standard temperature does not affect the duct leakage rates of 0.14 L/s/m², 0.62 L/s/m², and 2.48 L/s/m for tight and loose leakages. At standard temperature with duct leakage rate of 5.6 L/s/m², the fan capacity increased when the building leakage changed from tight to loose leakages. The airflow leaking from the stairwell and from the outside increased the duct leakages for loose building over tight building leakages.

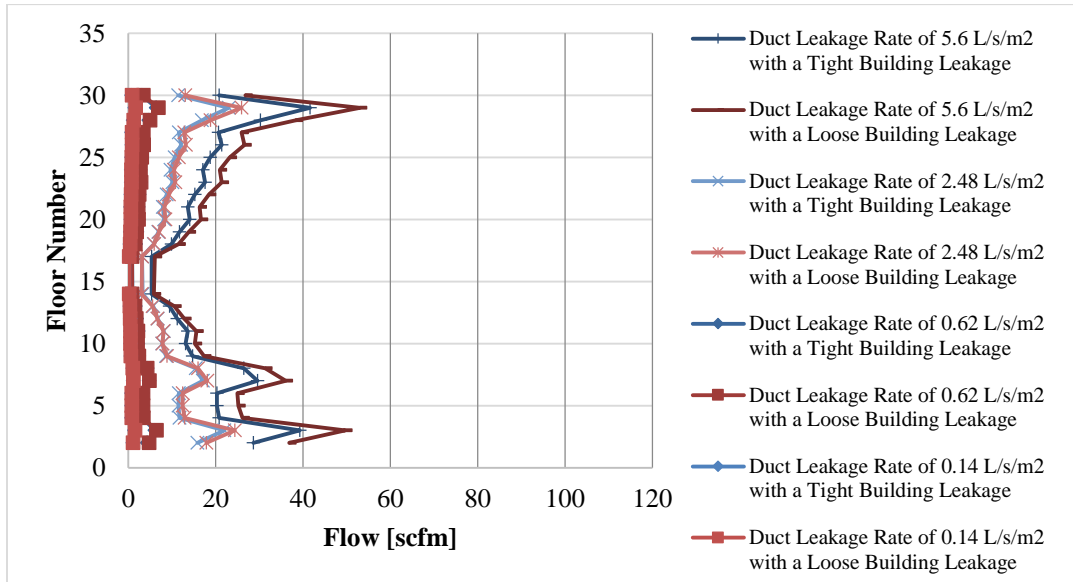


Figure 27: Airflow leakage from junction throughout Shaft_B during standard temperature for duct balance simulation.

The duct airflow leaking out of each junction during winter temperature (-20°C) is shown in Figure 28 for both tight and loose building leakages. The loose building leakages had a slightly higher air leakage than for the tight building leakages. As this figure showed there is no difference for loose and tight building leakages for duct leakage rates of 0.14 L/s/m^2 , 0.62 L/s/m^2 , 2.48 L/s/m^2 and 5.6 L/s/m^2 . The airflow leaking through the walls from the stairwell and the outside does not have any effect on the airflow leaking from the duct system.

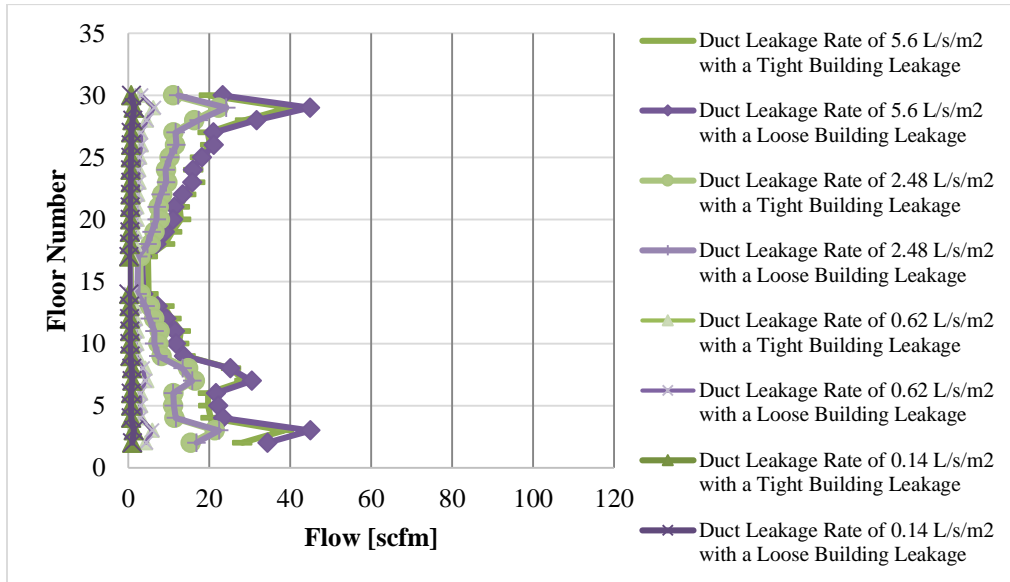


Figure 28: Airflow leakage from junction throughout Shaft_B during winter temperature for duct balance simulation.

6.4.3 Summary:

Sealed ducts had a small percent change in fan capacity, while unsealed ducts had an average change of 2% for both tight and loose building leakages. The difference between tight and loose building leakages, is roughly a 2% increase in total change of fan capacity. The difference in fan capacity from 20°C to either -20°C or 40°C is shown in Table 7. The duct balance method for the loose building leakages resulted in a greater change in fan capacity from standard temperature. The tight building leakages had roughly the same fan capacity for all temperatures, while the loose building leakages had the greatest fan capacity at 40°C.

Table 7: Summary of Stairwell_B fan capacity for duct balance simulation

Description	Outside Temperature	Duct Leakage Rate	Total Fan Capacity	Percent Change in Sealed Duct	Percent Change in Unsealed Duct	Total Percent Change	Difference in Fan Capacity From 20C	Percent Change in Fan Capacity From 20C			
	°C	L/s/m ²	m ³ /s								
Tight Building Leakage	Duct Balance Simulation Method	Stairwell_B	-20	0.14	4.61	1%	4.8%	0.26	6%		
				0.62	4.64			0.26	6%		
				2.48	4.73	2%		0.23	5%		
				5.6	4.83			0.23	5%		
			20	0.14	4.35	1%	5.9%				
				0.62	4.38						
				2.48	4.50	2%					
				5.6	4.61						
		40	0.14	4.40	1%	5.5%					
			0.62	4.43							
			2.48	4.53	2%				0.03	1%	
			5.6	4.64					0.03	1%	
		Loose Building Leakage	Duct Balance Simulation Method	Stairwell_B	-20	0.14	7.61	0.3%	2.7%	1.11	17%
						0.62	7.63			1.08	16%
						2.48	7.73	1%		1.12	17%
						5.6	7.81			1.08	16%
20	0.14				6.50	1%	3.7%				
	0.62				6.55						
	2.48				6.61	2%					
	5.6				6.74						
40	0.14			8.84	1%	2.7%					
	0.62			8.88							
	2.48			8.97	1%				2.33	36%	
	5.6			9.08					2.34	35%	

6.5 Single-Injection and Simple Air-Handle System Comparison:

The industry designer would model a stair pressurization system either by using a single-injection system or a simple air-handle system (AHS). Neither of these two systems used duct segments to transport air into the stairwell. The single-injection system had a single fan placed on the top of the stairwell that supplied outside air into the stairwell. The AHS had a fan located on the 3rd floor and another fan located on the 29th floor for both stairwell. Both the single and AHS provided a minimal door pressure difference of 0.10 inches of water for each simulation.

The results from Stairwell_A for a multiple-injection detailed duct system were compared to a single-injection system and an AHS, as shown in Table 8. The fan capacities for each steady state simulation method assessed at three different exterior temperatures and two building leakages were compared to the results from Table 4. The single injection system showed a fan capacity that is under pressurized at -20°C for tight building leakage and over pressurized for the rest of the condition compared to a detailed duct system. The AHS at 20°C and 40°C for both tight and loose building leakages showed similar result for fan capacity compared to a detailed duct system. The AHS at -20°C for both tight and loose building leakages had a fan capacity that were under pressurized. The change in fan capacity and the percent change in fan capacity for a single injection and AHS were compared to the detailed duct system, is also shown in Table 8.

Table 8: Fan capacity for high-rise building with single injection system and simple AHS system

		Single Injection - Fan Located on Roof			AHS - One fan located on the 3rd floor and the other located on the 29th floor		
Outside Temperature	Total Fan Capacity	Change in fan Capacity	Percent Change in Fan Capacity	Total Fan Capacity	Change in fan Capacity	Percent Change in Fan Capacity	
	m ³ /s			m ³ /s			
Stairwell_A – Tight Building Leakage	-20C	5.15	0.89	17%	4.94	1.10	22%
			0.96	19%		1.17	24%
			1.22	24%		1.43	29%
			1.60	31%		1.81	37%
	Average		23%		Average		28%
	20C	5.55	0.86	-15%	4.70	0.01	0%
			0.82	-15%		0.03	1%
			0.63	-11%		0.22	5%
			0.34	-6%		0.51	11%
	Average		-12%		Average		4%
	40C	5.58	0.18	-3%	5.66	0.26	-5%
			0.13	-2%		0.21	-4%
			0.08	1%		0.00	0%
0.42			7%	0.34		6%	
Average		1%		Average		-1%	
Stairwell_A – Loose Building Leakage	-20C	8.65	1.33	-15%	6.29	1.02	16%
			1.29	-15%		1.07	17%
			1.08	-12%		1.28	20%
			0.77	-9%		1.59	25%
	Average		-13%		Average		20%
	20C	9.40	2.96	-32%	6.64	0.21	-3%
			2.91	-31%		0.16	-2%
			2.75	-29%		0.01	0%
			2.47	-26%		0.29	4%
	Average		-29%		Average		0%
	40C	10.50	3.26	-31%	7.14	0.10	1%
			3.21	-31%		0.15	2%
			3.02	-29%		0.33	5%
2.73			-26%	0.62		9%	
Average		-29%		Average		4%	

The results from Stairwell_B for a multiple-injection detailed duct system were compared to a single-injection system and an AHS, as shown in Table 9. The fan capacities for each steady state simulation method assessed at three different exterior temperatures and two building leakages were compared to the results from Table 6. The single injection system showed a fan capacity that was under pressurized at -20°C for tight building leakage and were over pressurized for the rest of the condition compared to a detailed duct system. The AHS at 20°C and 40°C for a tight building leakages showed similar results for fan capacity compared to a detailed duct system. The AHS at -20°C for both tight and loose building leakages and 20°C and 40°C for both tight and loose building leakages showed a fan capacity that were under pressurized compared to a detailed duct system. The change in fan capacity and the percent change in fan capacity for a single injection and AHS were compared to the detailed duct system, is also shown in Table 9.

Table 9: Fan capacity for high-rise building with single injection system and simple AHS system

		Single Injection - Fan Located on Roof			AHS - One fan located on the 3rd floor and the other located on the 29th floor		
Outside Temperature	Total Fan Capacity	Change in fan Capacity	Percent Change in Fan Capacity	Total Fan Capacity	Change in fan Capacity	Percent Change in Fan Capacity	
	m ³ /s			m ³ /s			
Stairwell_B – Tight Building Leakage	-20C	5.10	0.49	10%	4.99	0.60	12%
			0.54	11%		0.65	13%
			0.63	12%		0.74	15%
			0.75	15%		0.86	17%
	Average		12%		Average		14%
	20C	5.13	0.74	-14%	4.40	0.01	0%
			0.72	-14%		0.01	0%
			0.61	-12%		0.11	3%
			0.49	-10%		0.24	5%
	Average		-12%		Average		2%
	40C	5.20	0.11	-2%	5.25	0.16	-3%
			0.08	-2%		0.14	-3%
0.04			1%	0.01		0%	
0.16			3%	0.11		2%	
Average		0%		Average		-1%	
Stairwell_B – Loose Building Leakage	-20C	9.15	1.58	-17%	4.39	3.19	73%
			1.58	-17%		3.19	73%
			1.46	-16%		3.31	75%
			1.34	-15%		3.43	78%
	Average		-16%		Average		75%
	20C	9.65	3.11	-32%	3.94	2.59	66%
			3.09	-32%		2.62	66%
			2.99	-31%		2.71	69%
			2.89	-30%		2.82	71%
	Average		-31%		Average		68%
	40C	10.80	3.48	-32%	4.06	3.26	80%
			3.46	-32%		3.29	81%
3.34			-31%	3.40		84%	
3.19			-30%	3.55		87%	
Average		-31%		Average		83%	

Chapter 7: Conclusion

A CONTAM model was used to evaluate the affects duct leakage had on a stairwell pressurization system. CONTAM is the network model that has been widely utilized for the analysis of smoke control systems, specifically to size fans for the stairwell pressurization system. This network model was used to determine if the pressurized system was capable of being balanced and perform as intended during a fire incident.

The following conclusions were drawn from this research:

1. The airflow leaking out of each duct system was affected by the air movement in the building, the building leakage and the temperature. Consideration of these parameters should be included in the calculation of fan capacity for pressurized systems used in multi-story buildings.
2. The results showed that duct balance simulation methods provided the most accurate means to determine the loss coefficients for the duct systems. The results also showed that the final calculation for fan capacities were obtained by using the steady state simulation methods with these coefficients.
3. The steady state simulation method for a tight building leakage had a significant increase in fan capacity of 11% when surrounded by all interior walls and exterior temperature of 20°C compared to Stairwell_B. However, when the stairwell was surrounded by two exterior and two interior walls with an exterior temperature of 20°C, there was an increase in fan capacity of only 5.5% compared to Stairwell_A. When the stairwell was surrounded by all interior

walls with an exterior temperature of 20°C, the data showed that a loose building leakage had a significant increase in fan capacity of 8% compared to Stairwell_B. The increase in fan capacity was lowered to 4% for the same leakage and exterior temperature, but the stairwell was surrounded by two exterior and two interior walls compared to Stairwell_A.

4. As expected, this research showed that a loose building leakage effects had a greater fan capacity than a building with a tight building leakage. The change in fan capacity from 20°C to -20°C increased by 28% for tight building leakage for both stairwells, while the change of exterior temperature from 20°C to 40°C increased fan capacity by only 16%. These results showed that temperature had a significant affect on the required fan capacity to pressurize a tight building leakage condition. The change in fan capacity, when the exterior temperature changed from 20°C to -20°C, increased by 15% for loose building leakage for both stairwells. When the temperature changed from 20°C to 40°C, the change in fan capacity increased by 12%, which was slightly less. The tight building leakage showed a similar increase in fan capacity required to pressurize each stairwell.
5. The research showed the importance of knowing the type of duct systems, sealed or unsealed, when analyzing pressurized systems for multi-story buildings, so not to over or under size fan capacity.

These conclusions resulting from this research were based on a 31 story residential building with various floor heights, floor layouts and a multi-injection system. The applicability of these results to pressurization systems in other buildings is unknown, but this research provided important insight in pressurization of stairwells for multi-story building. For example, air movement in the building, type of building leakage, duct type, type of floor plans, location of the stairwell and outside temperature are demonstrated to be important factors for the sizing of an air delivery system.

Chapter 8: Suggestions for Further Study

This study has identified several areas where additional research will help to improve the design of stairwell pressurization systems. The following future research should be considered:

1. Consider a high-rise building with a generic floor plan to evaluate the leakage out of a duct system between an open floor plan and a partition floor plan with a stairwell surround by all standard temperature. Then study the effects on a stairwell located in the corner of the building. Compare the results from the model to pressurization systems currently used in high-rise buildings.
2. Evaluate the placement of the mechanical shaft to the stairwell by examining the airflow transferring from the stairwell into the mechanical shaft. Investigate the effects pressure difference in the mechanical shaft has on duct leakage.
3. Evaluate the effects on heating and cooling outside air for high-rise multiple-injection pressurization systems.
4. Collect data in an actual building and compare to CONTAM results.

Appendix A

Floor plan images used to construct a CONTAM model.

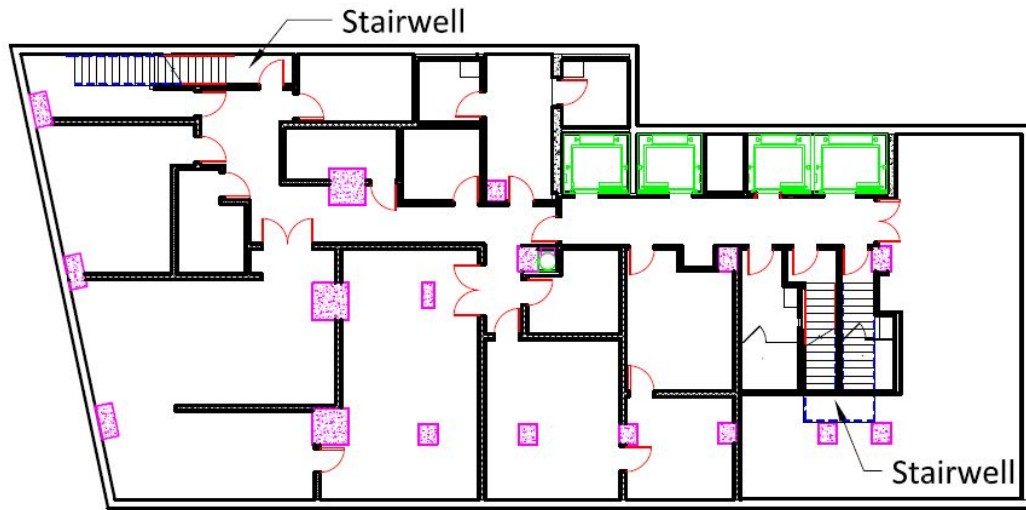


Figure A - 1: Basement level

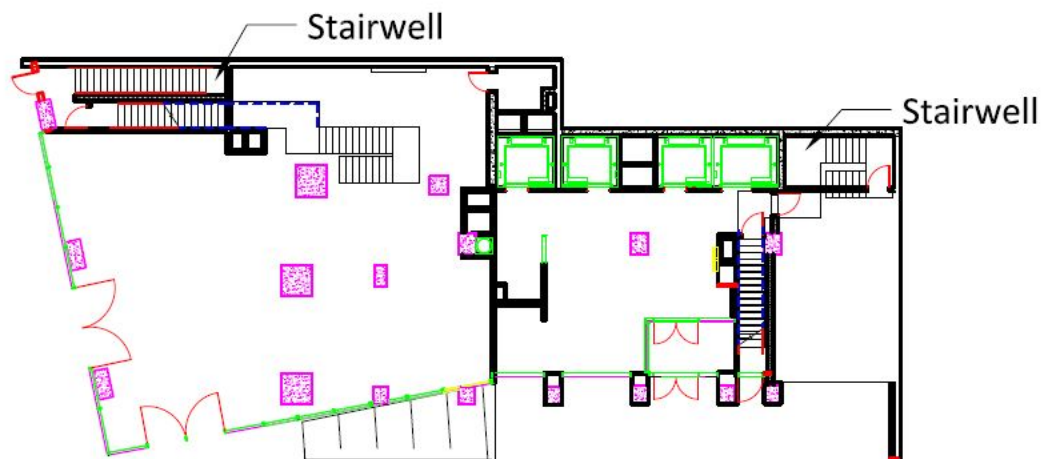


Figure A - 2: Ground Floor

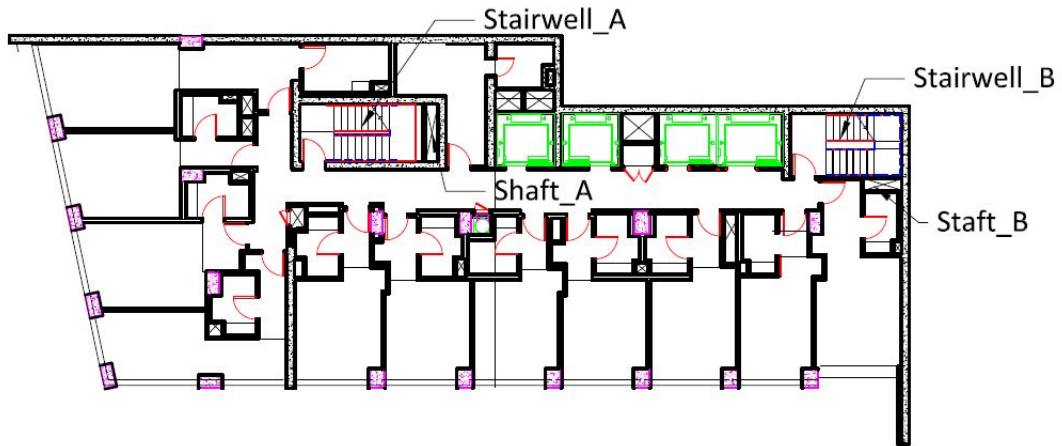


Figure A - 3: 2nd floor layout has 12 bedrooms and 12 bathrooms

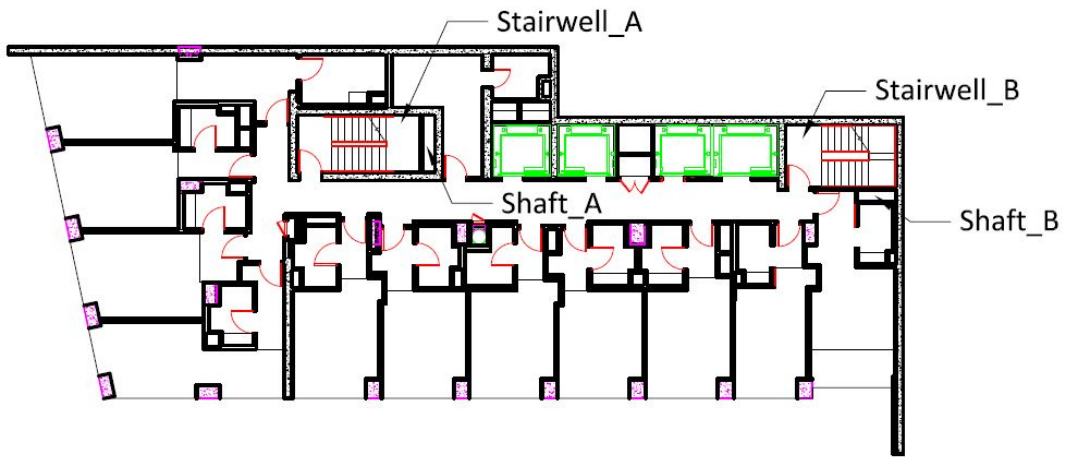


Figure A - 4: 3rd through 5th floor layout has 12 bedrooms and 12 bathrooms

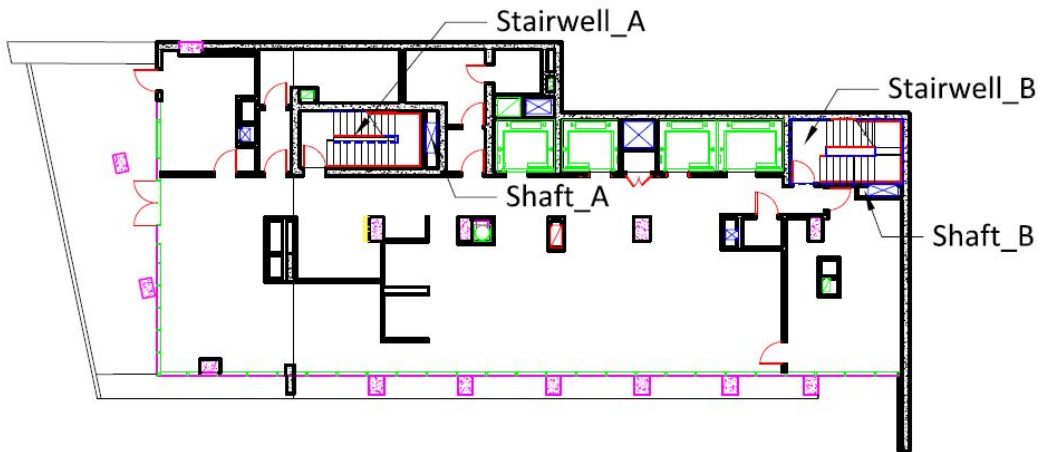


Figure A - 5: 6th floor has an open floor layout for hotel kitchen and dining area

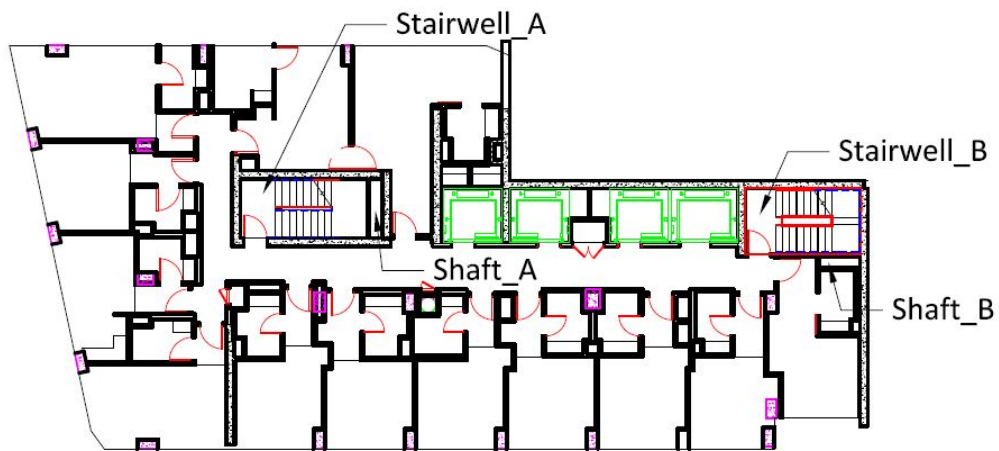


Figure A - 6: 18th through 27th floors layout has 13 bedrooms and 13 bathrooms

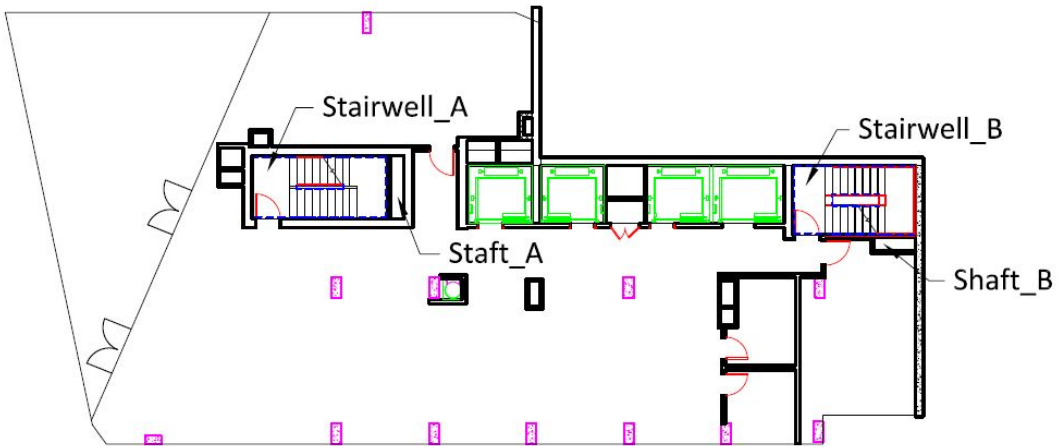


Figure A - 7: 28th floor has an open floor layout for restaurant and bar usage.

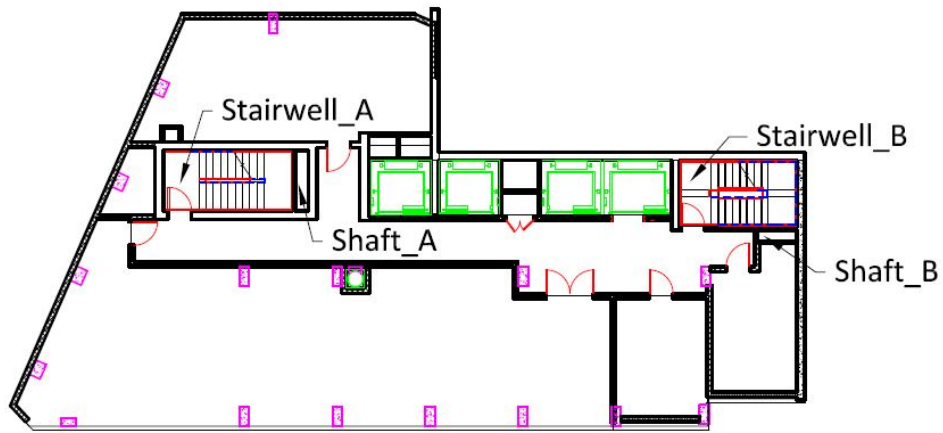


Figure A - 8: 29th floor has an open layout for mechanical equipment.

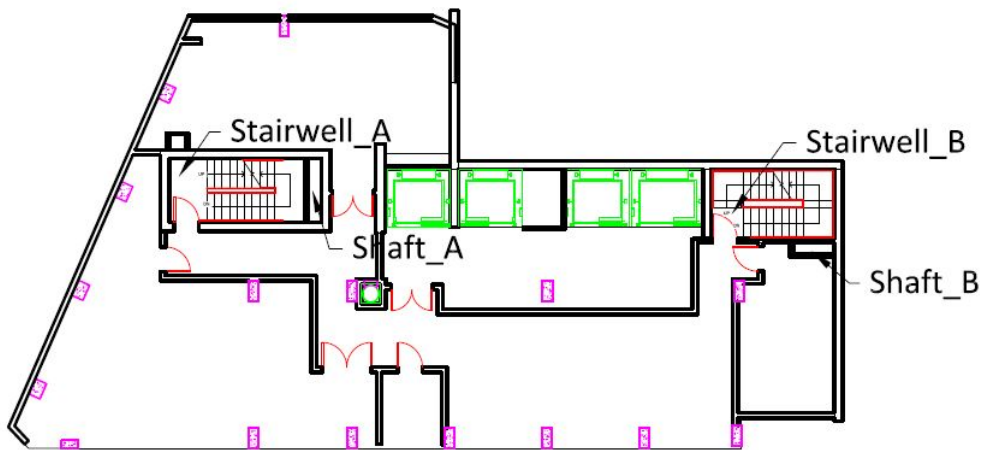


Figure A - 9: 30th floor has an open layout for mechanical equipment.

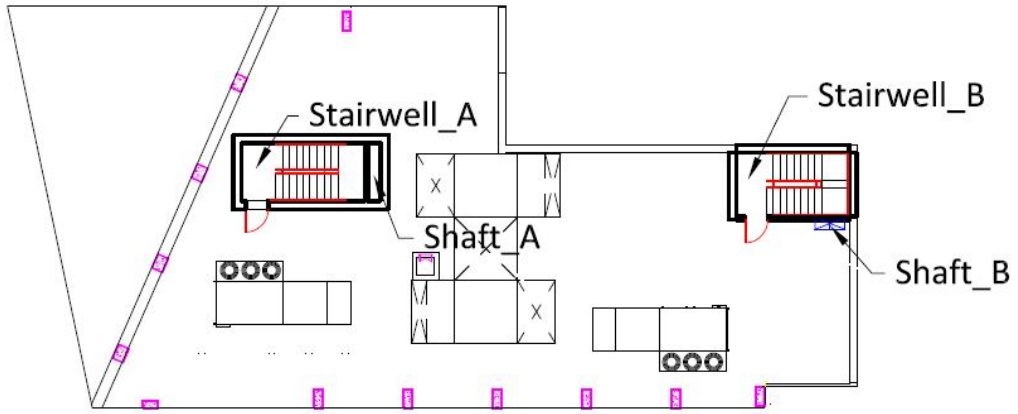


Figure A - 10: Roof floor plan showing stairwells and shafts exposed to exterior conditions.

Table A - 1: Elevation and floor height of the residential building

Name	Elevation (m)	Height (m)
Basement level	-3.7	3.66
Ground Floor	0	6.71
2nd Floor	6.71	2.95
3rd Floor	9.66	2.95
4th Floor	12.61	2.95
5th Floor	15.56	3.96
6th Floor	19.52	6.4
7th Floor	25.92	2.95
8th Floor	28.87	2.95
9th Floor	31.82	2.95
10th Floor	34.77	2.95
11th Floor	37.72	2.95
12th Floor	40.67	2.95
13th Floor	43.62	2.95
14th Floor	46.57	2.95
15th Floor	49.52	2.95
16th Floor	52.47	2.95
17th Floor	55.42	2.95
18th Floor	58.37	2.95
19th Floor	61.32	2.95
20th Floor	64.27	2.95
21st Floor	67.22	2.95
22nd Floor	70.17	2.95
23rd Floor	73.12	2.95
24th Floor	76.07	2.95
25th Floor	79.02	2.95
26th Floor	81.97	2.95
27th Floor	84.92	4.88
28th Floor	89.8	4.88
29th Floor	94.68	3.51
30th Floor	98.19	3.51
Roof	101.7	3.3
Bulkhead Roof	105	3.3

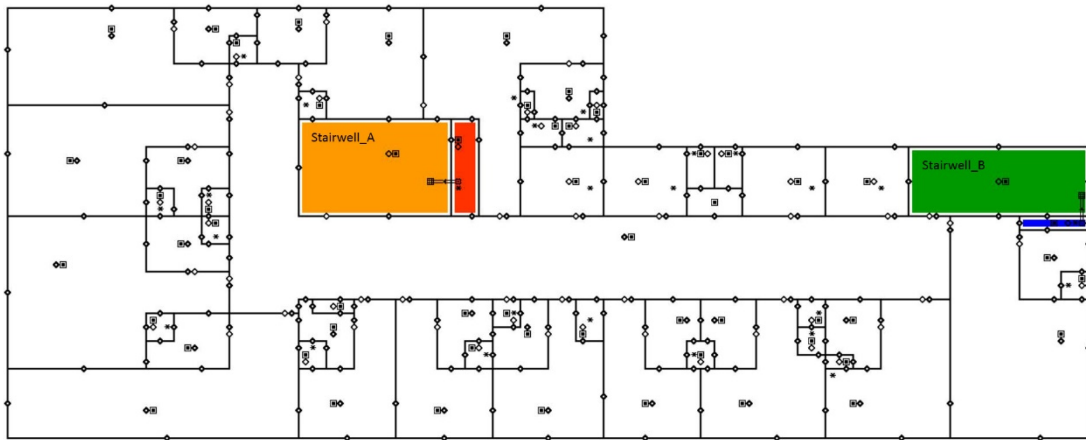


Figure A - 11: CONTAM model 7th through 17th floors showing location of stairwells and duct shafts.

Appendix B

The following graphs show the stairwell door pressure difference for both Stairwell_A and Stairwell_B. Each graph showed that the different duct leakage rates affects on stairwell door pressure difference at a constant temperature and building leakage. The classifications relate to the following duct leakage rates:

- Classification 4 relates to duct leakage rate of 0.14 L/s/m²
- Classification 17 relates to duct leakage rate of 0.62 L/s/m²
- Classification 68 relates to duct leakage rate of 2.48 L/s/m²
- Classification 155 relates to duct leakage rate of 5.6 L/s/m²

Duct Balance Simulation Method

Figures B - 1 through B - 12 show the door pressure difference for Stairwell_A using the steady state method.

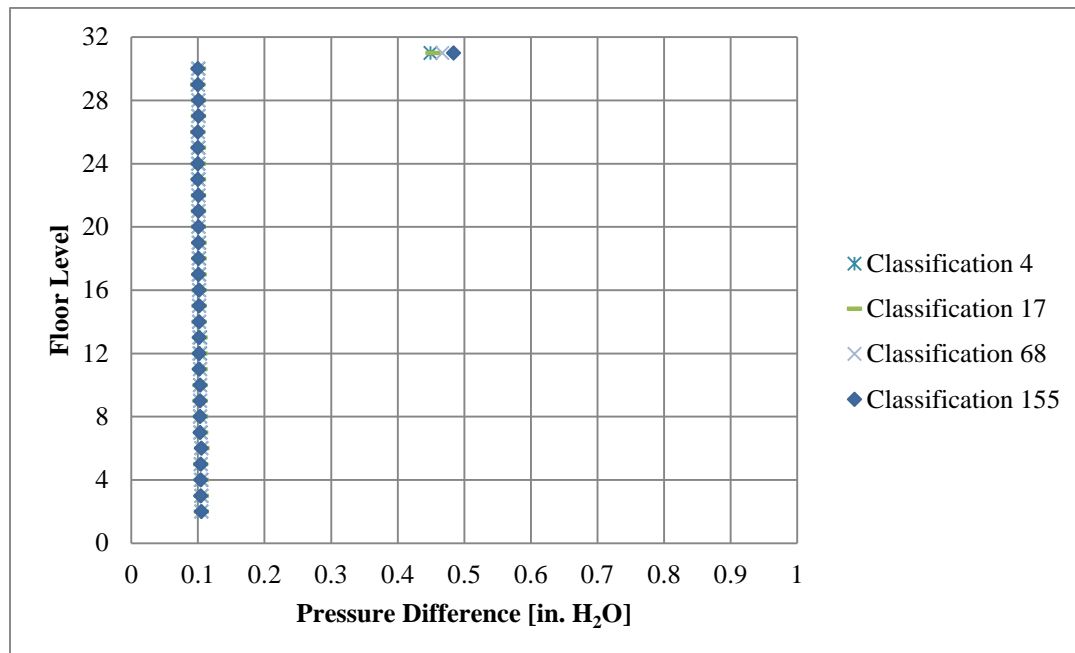


Figure B - 1: Shows the door pressure difference for Stairwell_A with outside temperature at 20C and a tight wall leakage using the duct balance simulation.

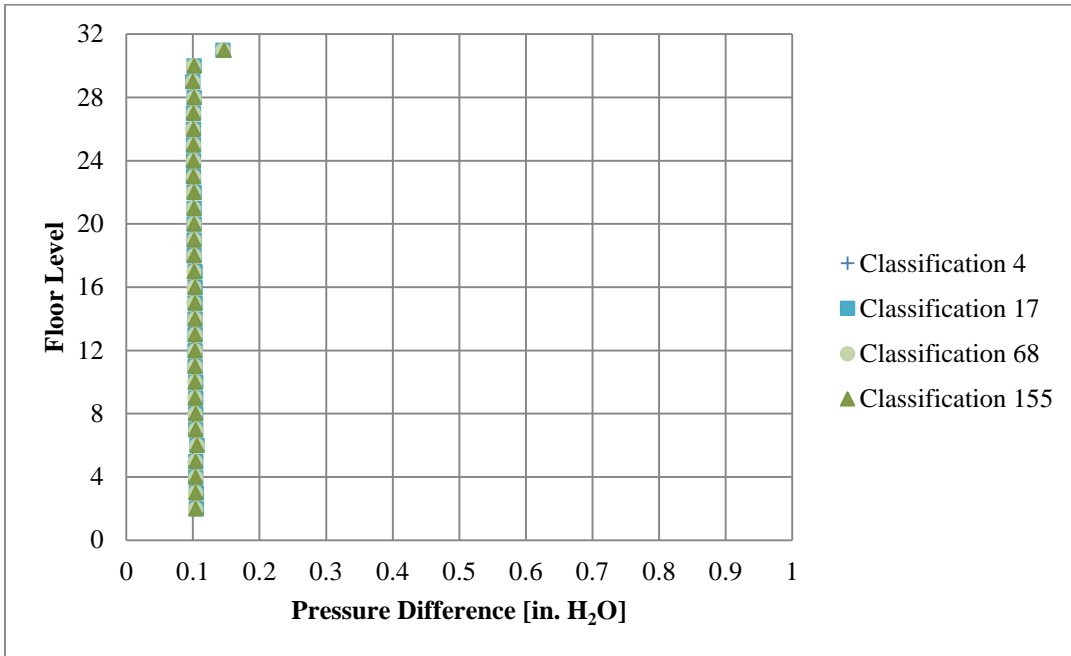


Figure B - 2: Shows the door pressure difference for Stairwell_A with outside temperature at 20C and a loose wall leakage using the duct balance simulation

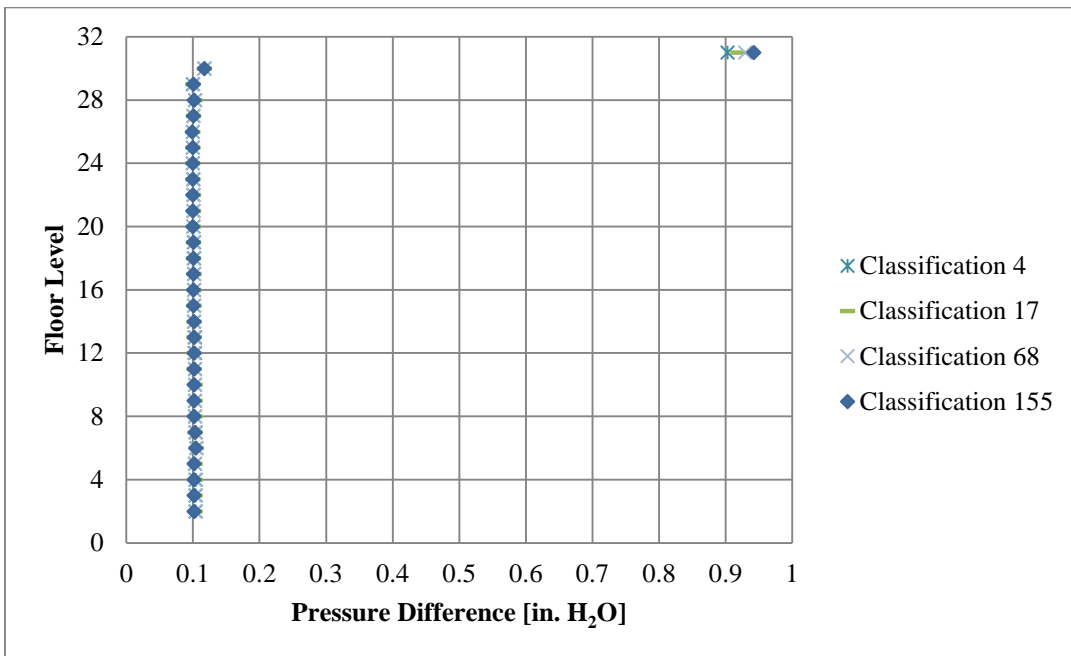


Figure B - 3: Shows Stairwell_A door pressure differences at -20C for a tight wall leakage using the duct balance simulation method.

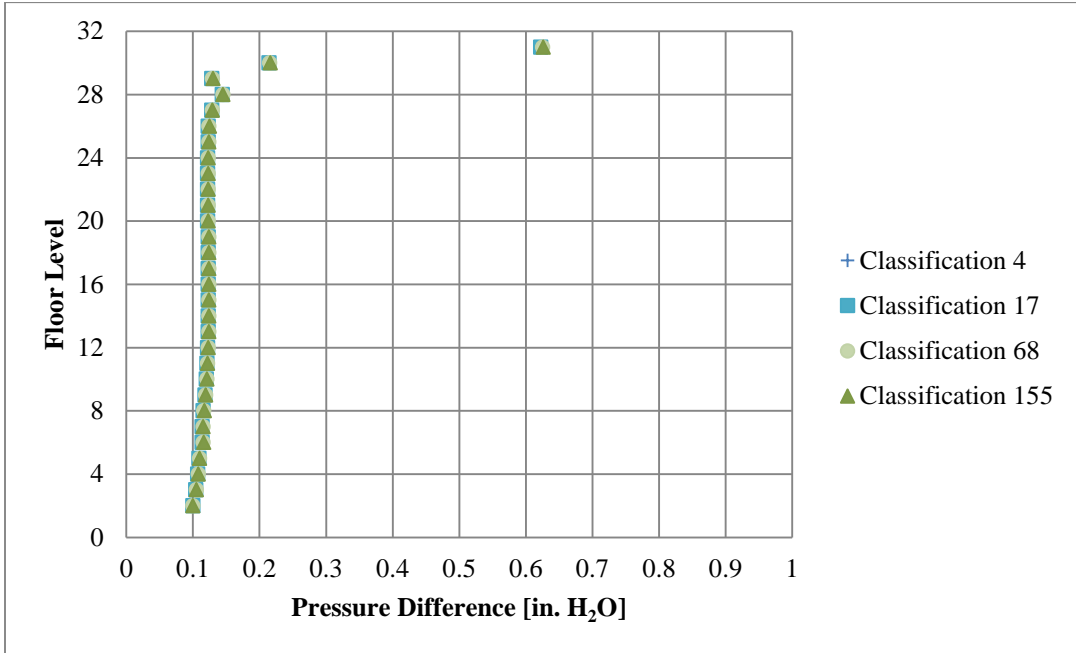


Figure B - 4: Shows the door pressure difference for Stairwell_A at -20C a loose wall leakage using the duct balance simulation

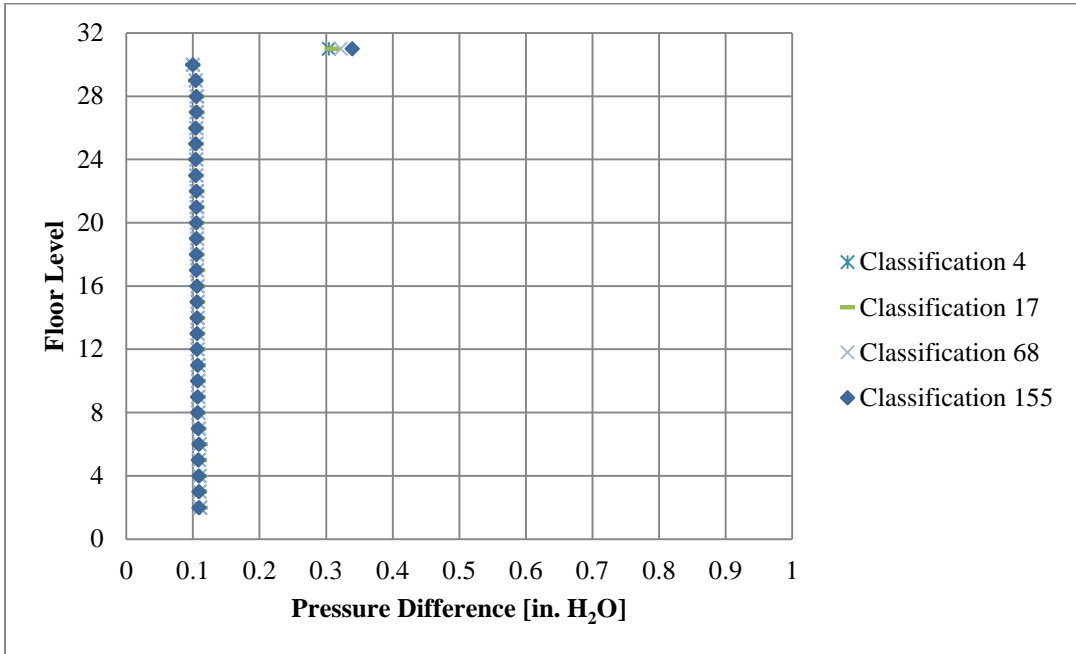


Figure B - 5: Shows Stairwell_A door pressure differences at 40C for a tight wall leakage using the duct balance simulation method.

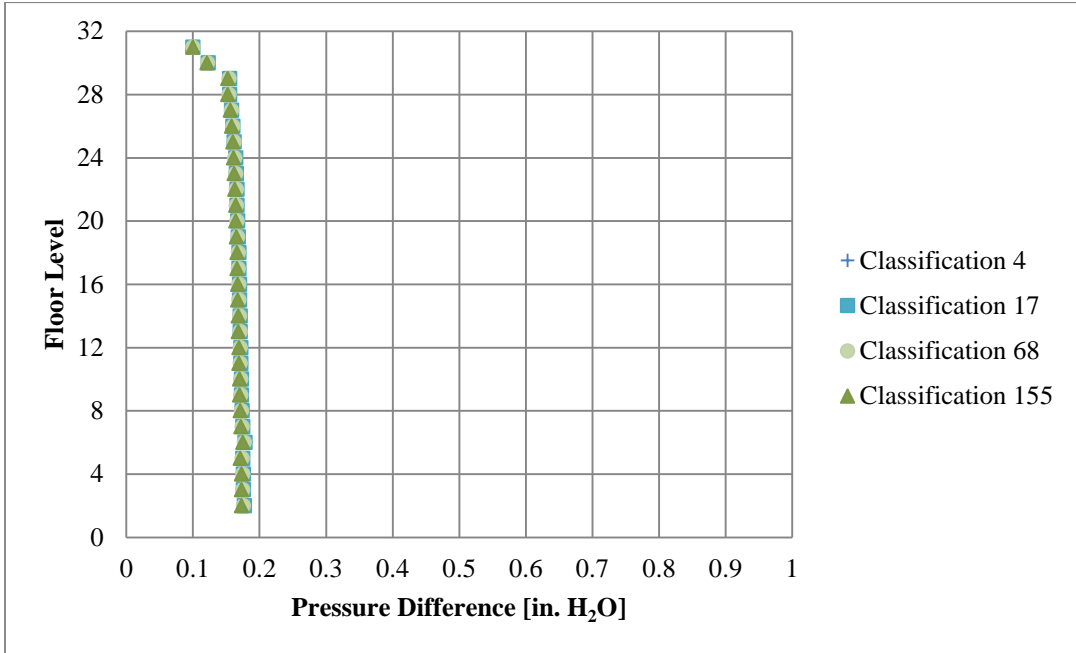


Figure B - 6: Shows the door pressure difference for Stairwell_A at 40C a loose wall leakage using the duct balance simulation.

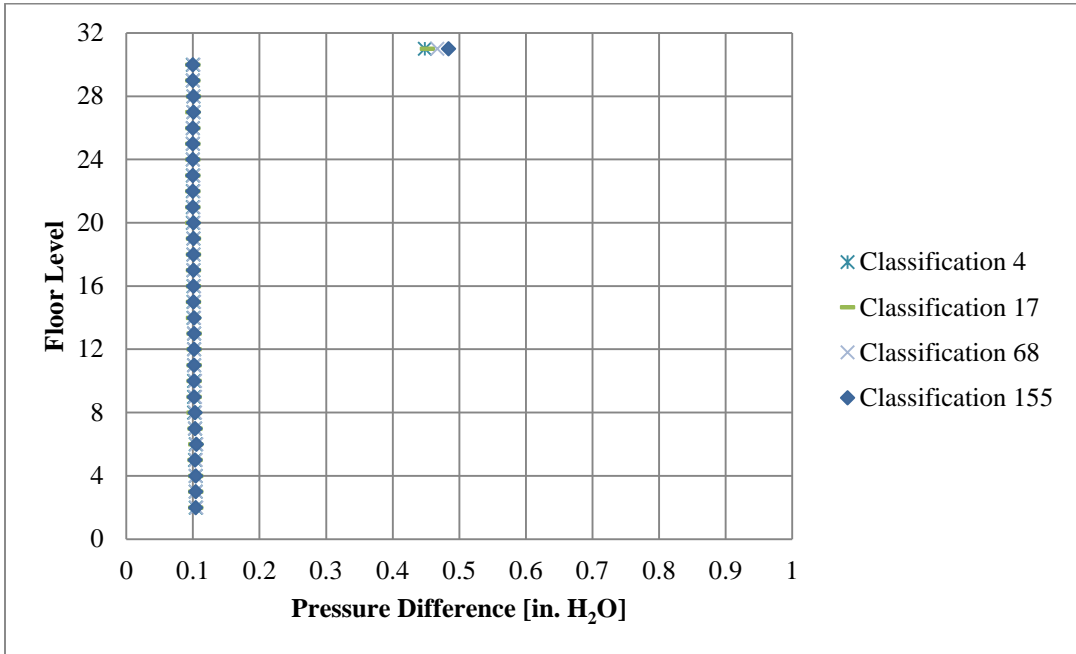


Figure B - 7: Shows Stairwell_B door pressure differences at 20C for a tight wall leakage using the duct balance simulation method.

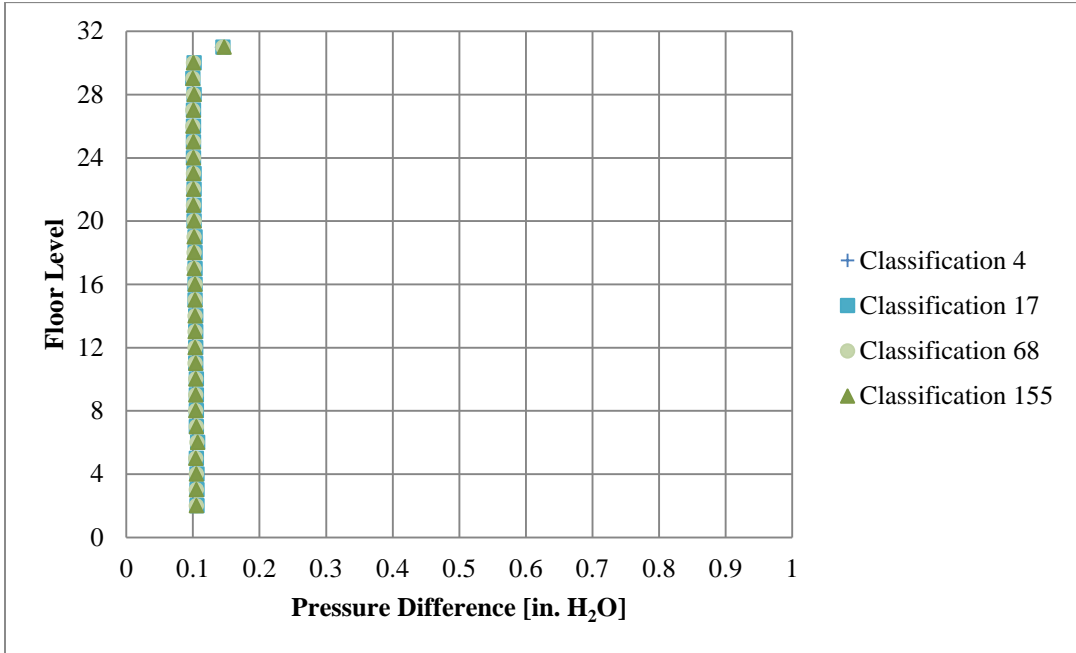


Figure B - 8: Shows Stairwell_B door pressure differences at 20C for a loose wall leakage using the duct balance simulation method.

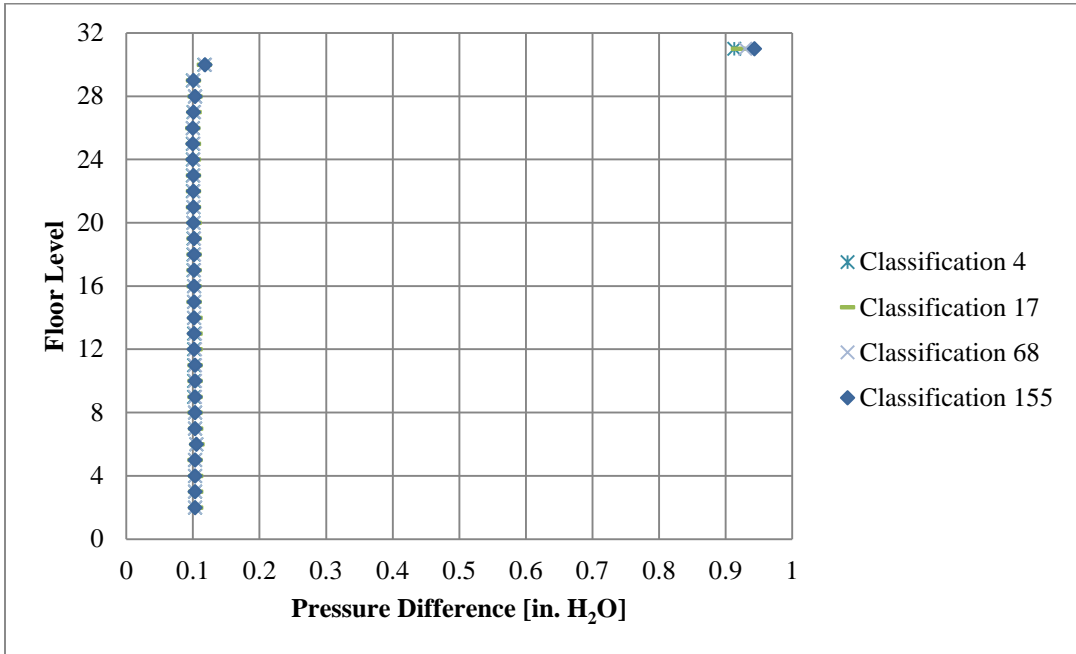


Figure B - 9: Shows Stairwell_B door pressure differences at -20C for a tight wall leakage using the duct balance simulation method.

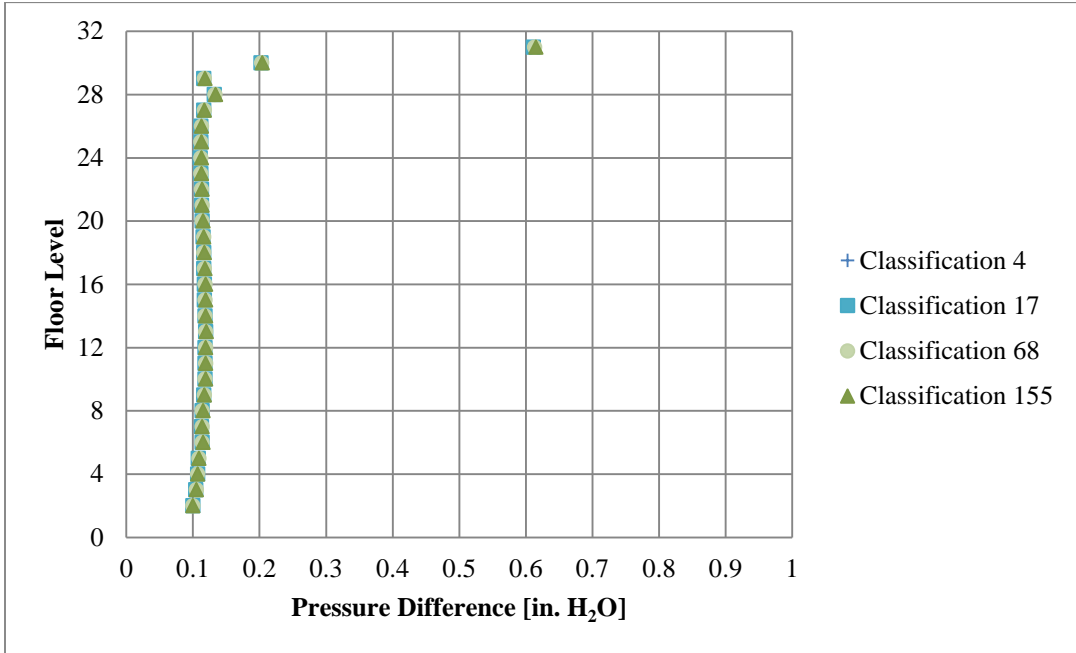


Figure B - 10: Shows Stairwell_B door pressure differences at -20C for a loose wall leakage using the duct balance simulation method.

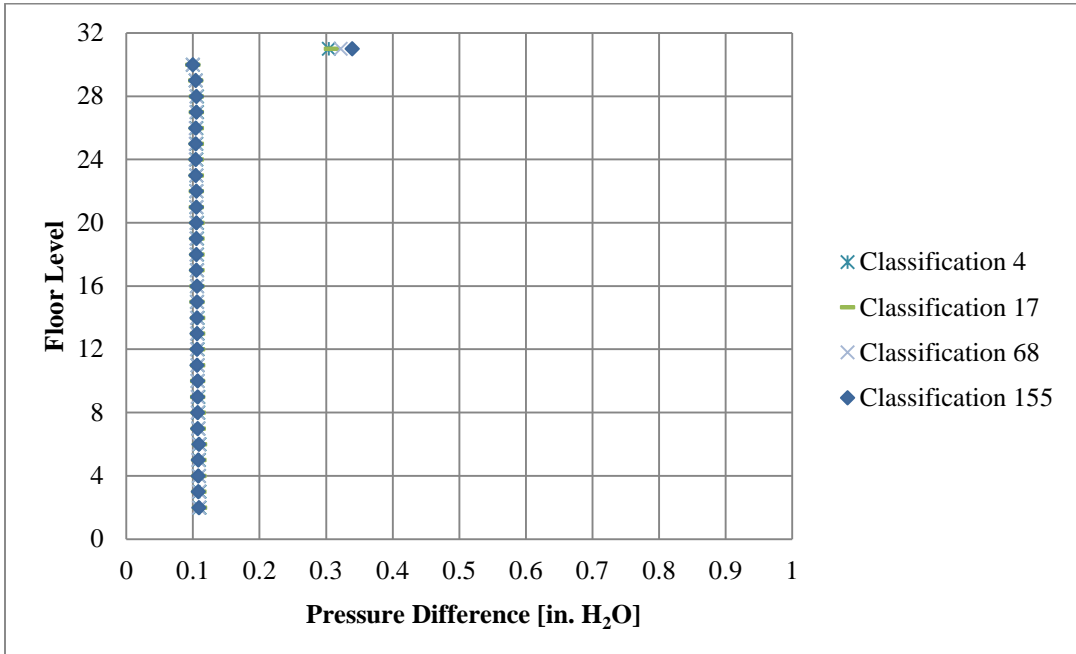


Figure B - 11: Shows Stairwell_B door pressure differences at 40C for a tight wall leakage using the duct balance simulation method.

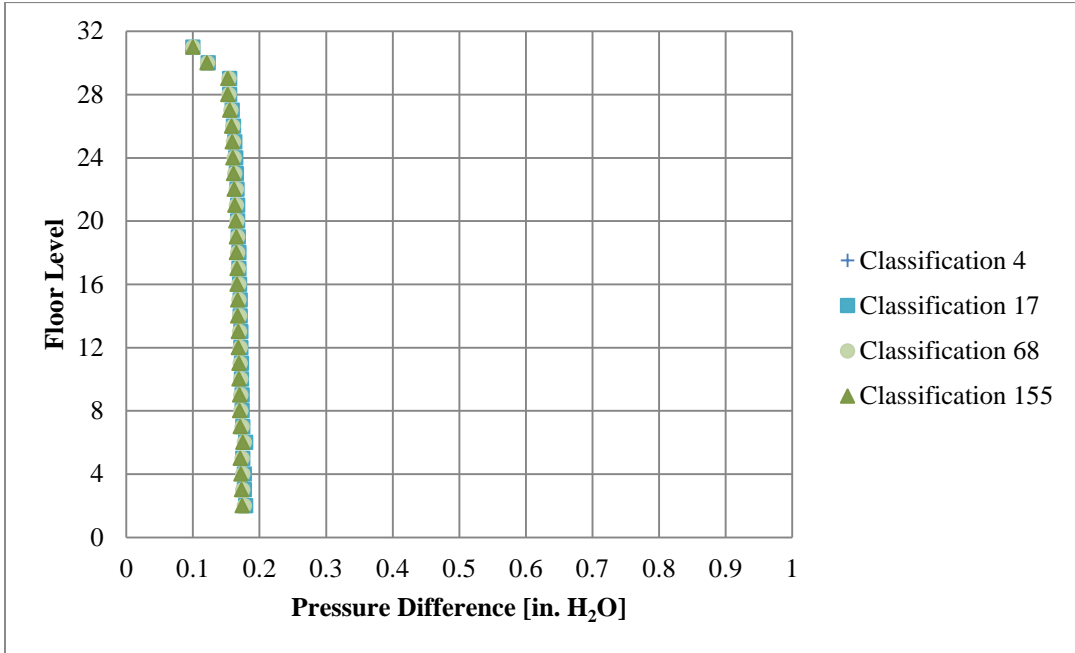


Figure B - 12: Shows Stairwell_B door pressure differences at 40C for a loose wall leakage using the duct balance simulation method.

Steady State Simulation Method

Figures B - 13 through B - 24 show the door pressure difference for Stairwell_A using the steady state method.

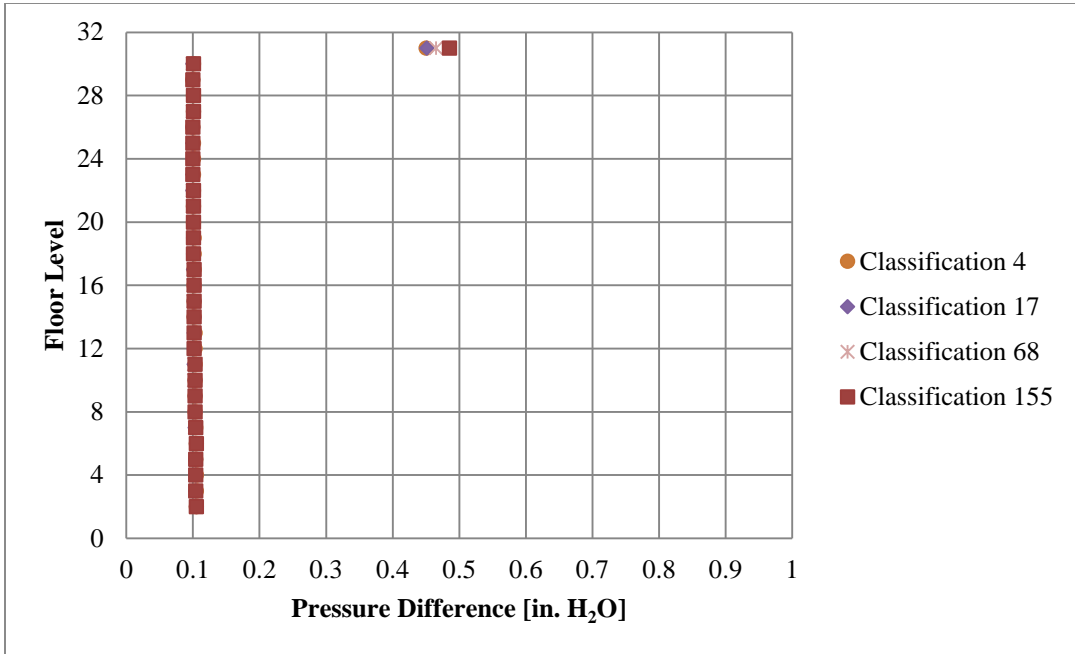


Figure B - 13: Shows Stairwell_A door pressure differences at 20C for a tight wall leakage using the steady state simulation method.

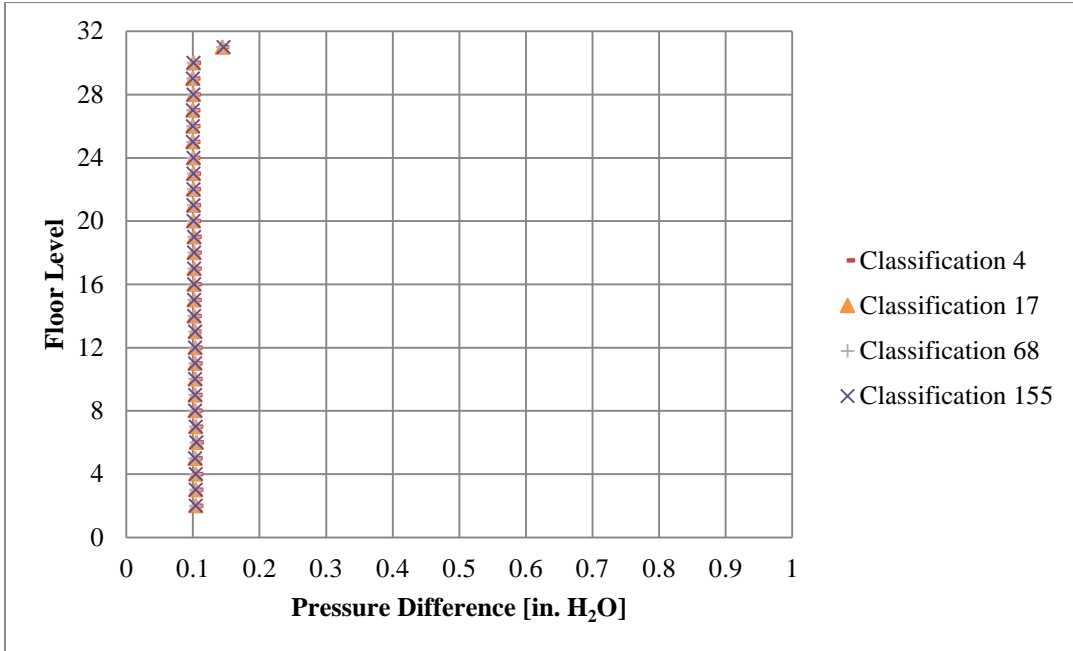


Figure B - 14: Shows Stairwell_A door pressure differences at 20C for a loose wall leakage using the steady state simulation method.

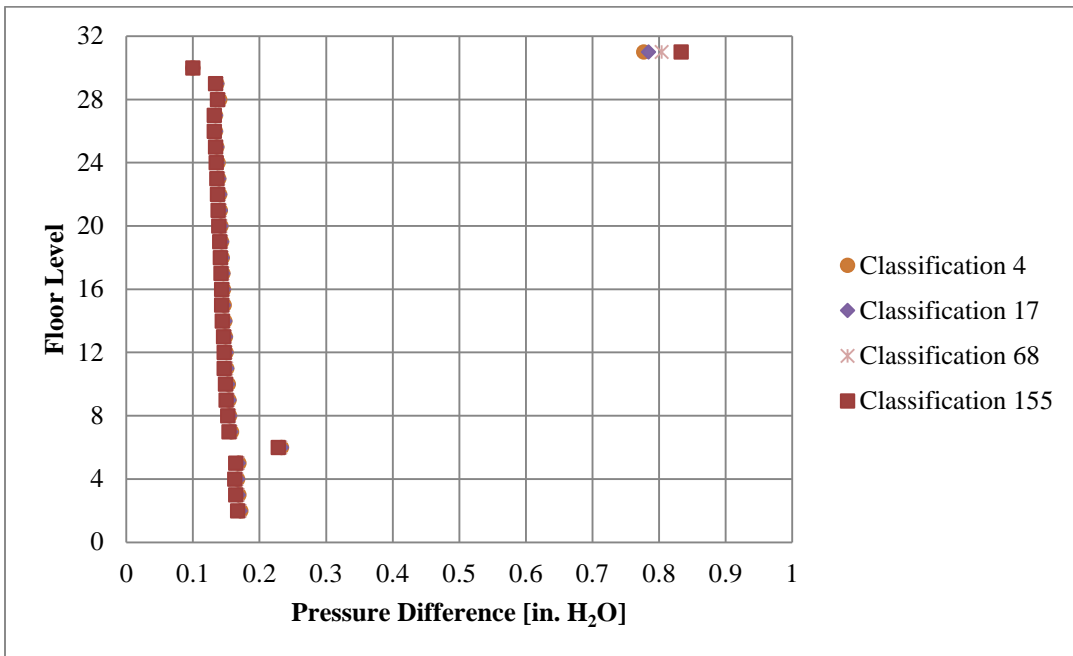


Figure B - 15: Shows Stairwell_A door pressure differences at -20C for a tight wall leakage using the steady state simulation method.

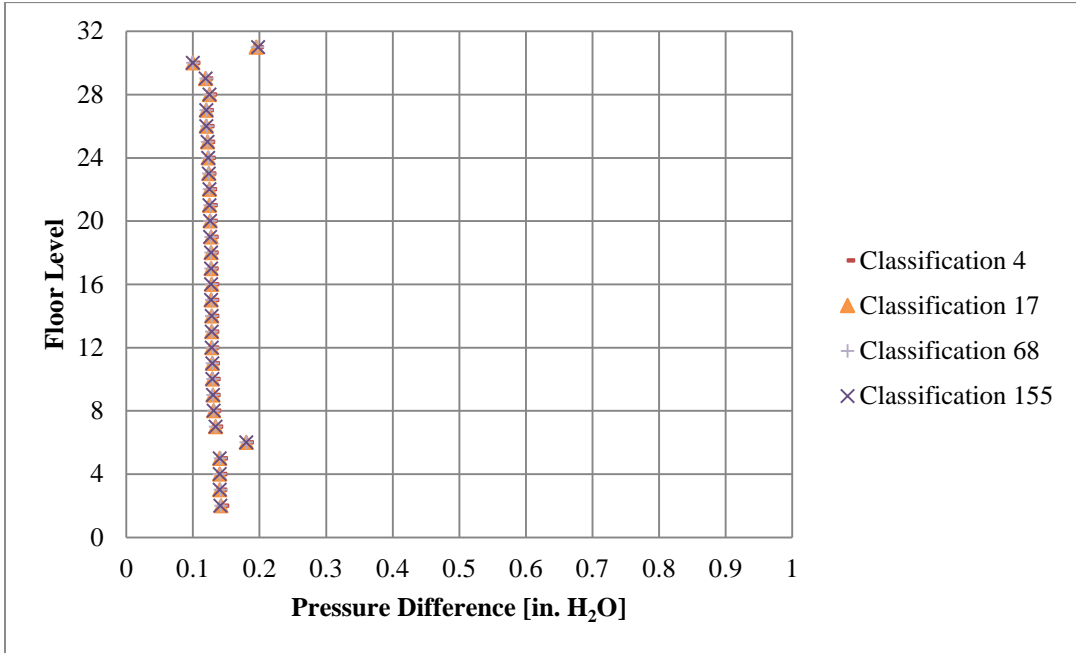


Figure B - 16: Shows Stairwell_A door pressure differences at -20C for a loose wall leakage using the steady state simulation method.

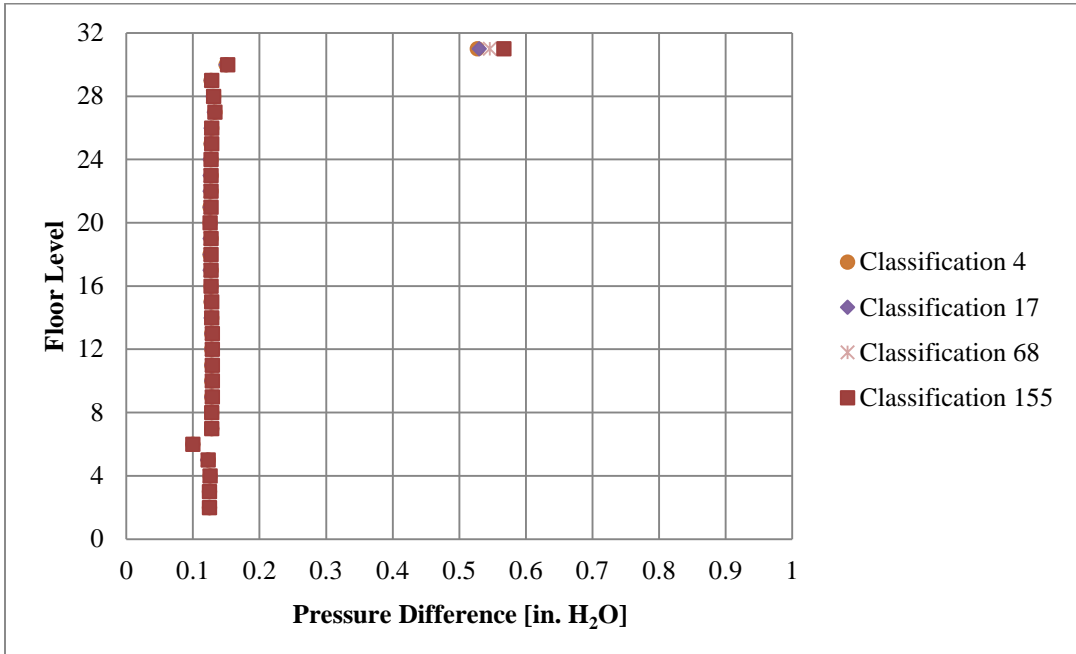


Figure B - 17: Shows Stairwell_A door pressure differences at 40C for a tight wall leakage using the steady state simulation method.

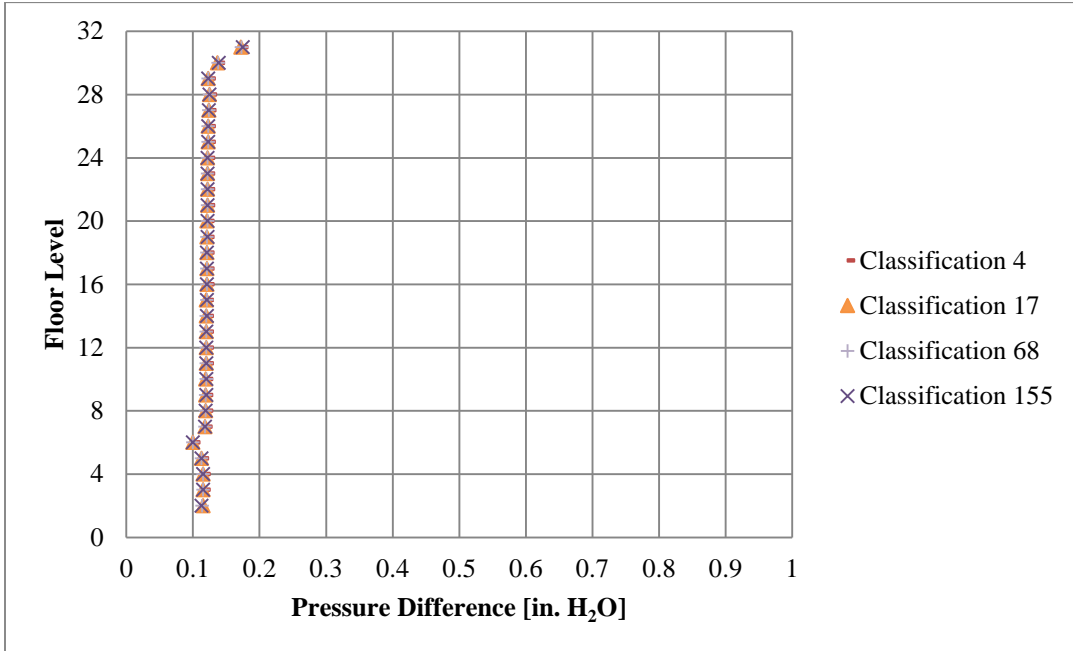


Figure B - 18: Shows Stairwell_A door pressure differences at 40C for a loose wall leakage using the steady state simulation method.

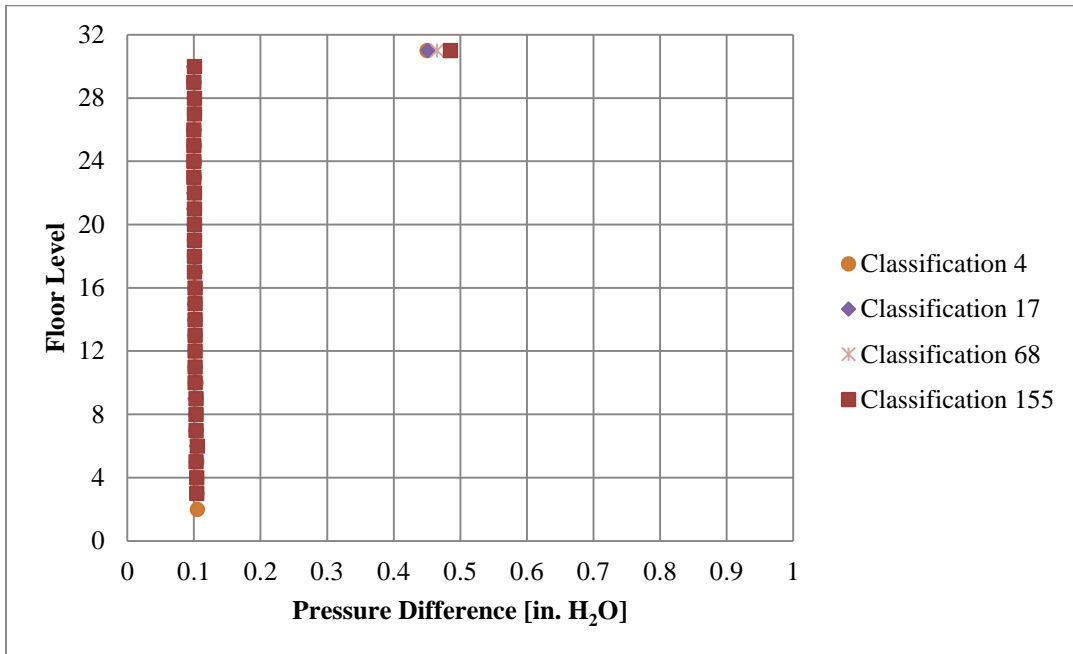


Figure B - 19: Shows Stairwell_B door pressure differences at 20C for a tight wall leakage using the steady state simulation method.

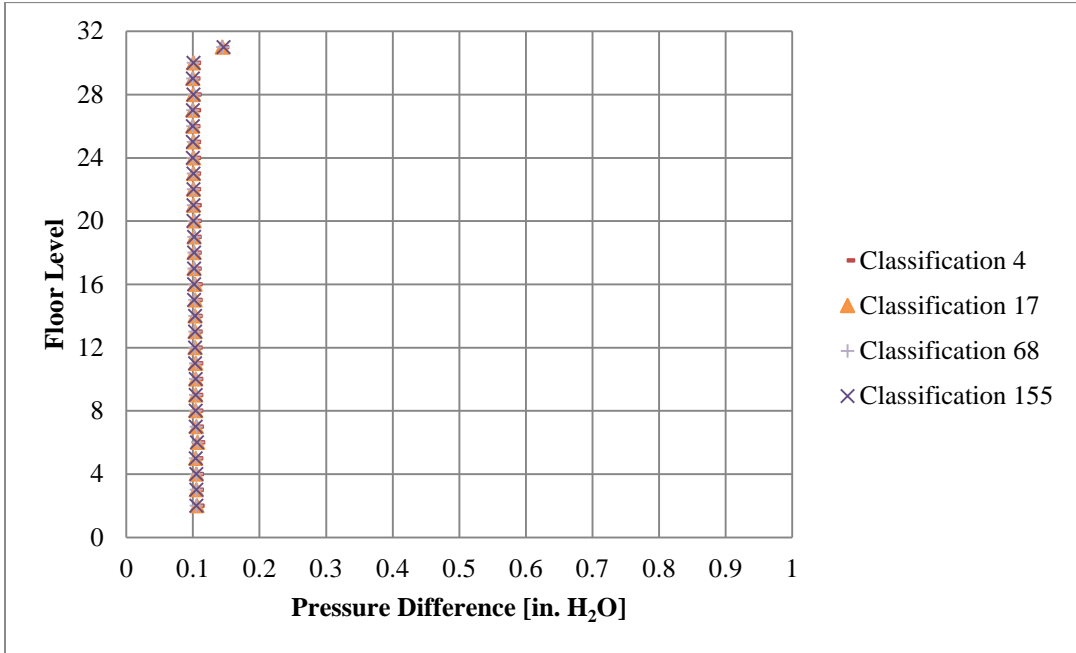


Figure B - 20: Shows the door pressure difference for Stairwell_B at 20C a loose wall leakage using the steady state simulation method

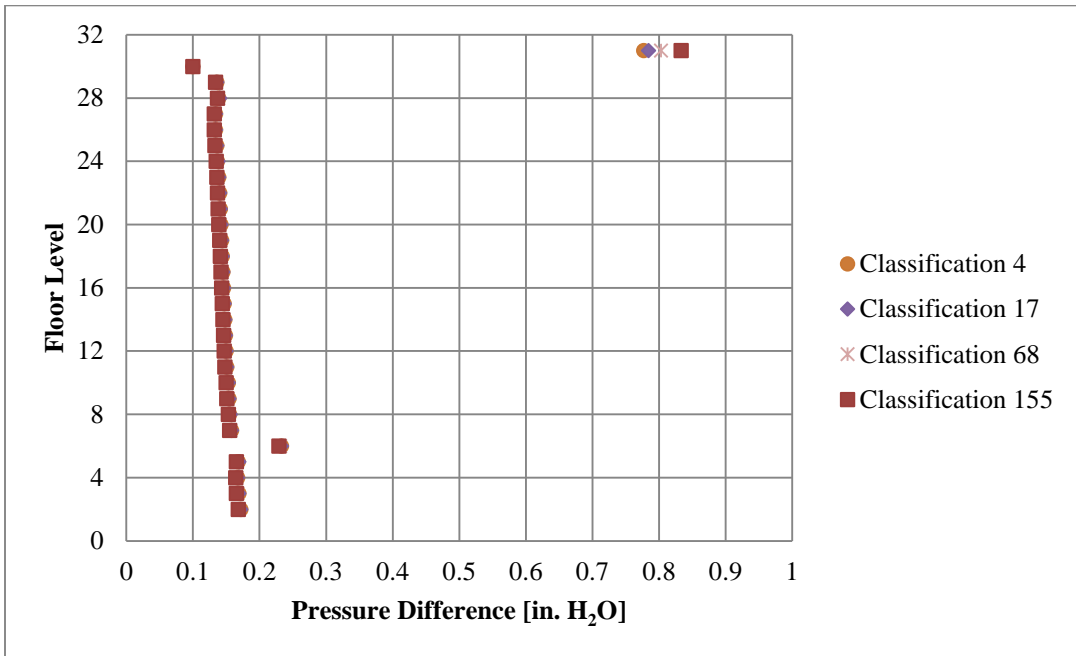


Figure B - 21: Shows Stairwell_B door pressure differences at -20C for a tight wall leakage using the steady state simulation method.

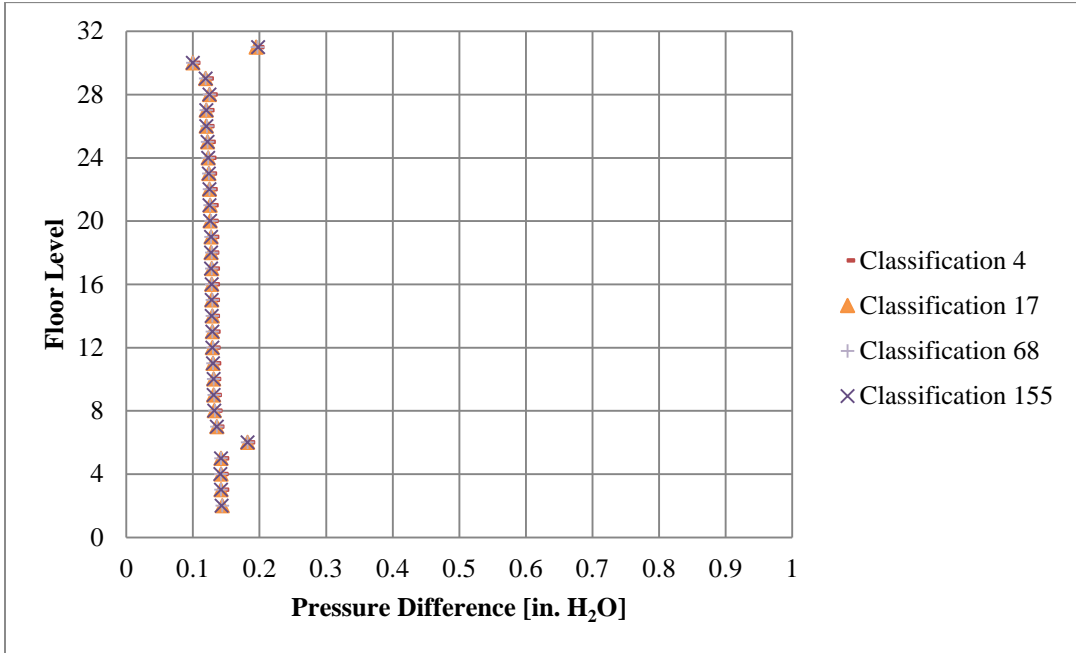


Figure B - 22: Shows the door pressure difference for Stairwell_B at -20C a loose wall leakage using the Steady State simulation Method

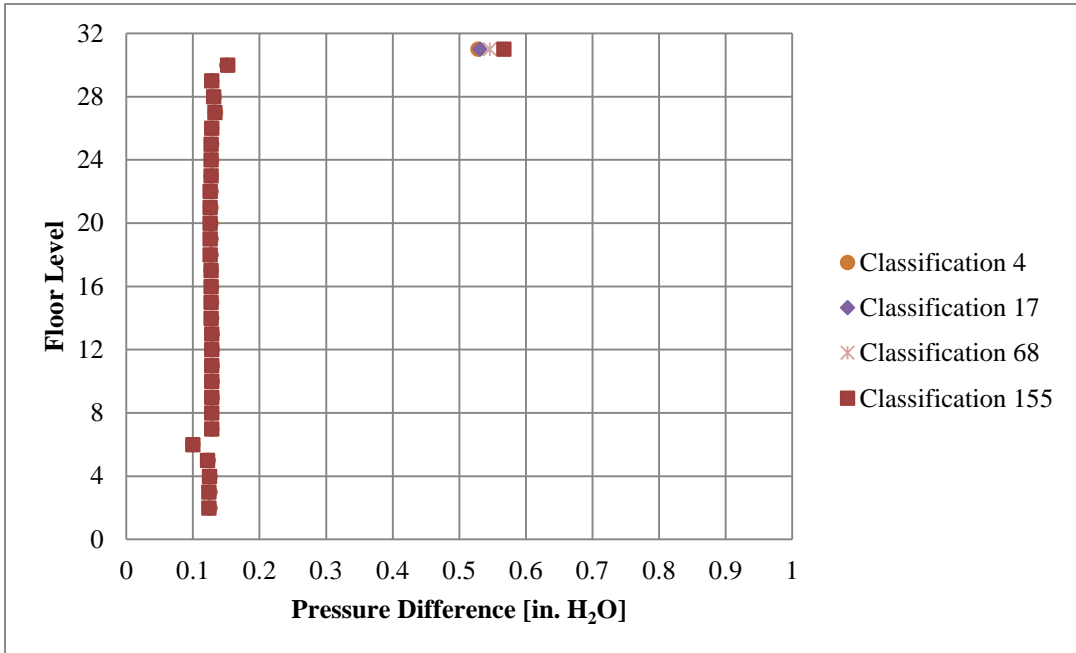


Figure B - 23: Shows Stairwell_B door pressure differences at 40C for a tight wall leakage using the steady state simulation method.

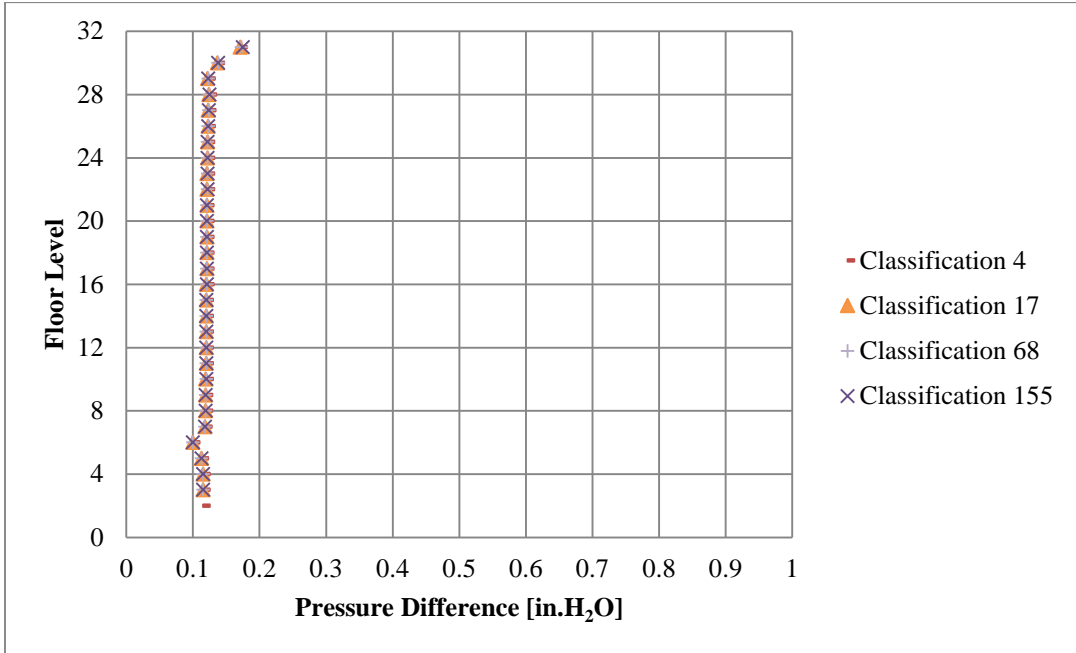


Figure B - 24: Shows the door pressure difference for Stairwell_B at 40C for a loose wall leakage using the Steady State simulation Method

Bibliography

- [1] J. Tubbs, M. Johann and A. Neviackas, *Smoke Control for Tall Buildings - An Integrated Approach to Life Safety*, ASHRAE Transactions, 2011, pp. 470-477.
- [2] J. H. Klote, *Smoke Control*, 4th ed., Quincy, Massachusetts: National Fire Protection Association, 2012, pp. 4-367 - 4-286.
- [3] J. R. Hall, Quincy, MA: National Fire Protection Association, 2011.
- [4] Y. Wang and F. Gao, *Tests of Stairwell Pressurization Systems for Smoke Control In a High-Rise Building*, vol. 119, ASHRAE Transactions, 2004, pp. 185-193.
- [5] G. N. Walton and S. W. Dols, *CONTAM*, Gaithersburg, Maryland: National Institute of Standards and Technology, 2013.
- [6] "ASHRAE," in *2009 ASHRAE Handbook - Fundamentals (SI Edition)*, 2009 ed., American Society of Heating, Refrigerating and Air-Conditioning Engineers, Inc., 2009.
- [7] *NFPA 92*, 2012 ed., Quincy, MA: National Fire Protection Association, 2013.
- [8] AISI and SMACNA, *Measurements and analysis of leakage rates from seams and joints of air handling systems*, Chantilly, VA: American Iron and Steel Institute and Sheet Metal and Air Conditioning Contractors' National Association, 1972.
- [9] Swim and Griggs, "DUCT LEAKAGE MEASUREMENT AND ANALYSIS," in *ASHRAE Transactions* , 1995.
- [10] K. Maatouk, *Investigation of Airflow Patterns Inside Tall Buildings*, vol. 3, Bentham Science Publisher Ltd. , 2008, pp. 65-70.

- [11] E. Anderson, *Smoke Control in Very Tall Building - Past, Present, and Future*, Fire Protection Engineering Magazine, 2013.
- [12] A. K. Persily, "Myths About Building Envelopes," *ASHRAE JOURNAL*, pp. 39-45, March 1999.
- [13] G. N. Walton, "AIRNET - A Computer Program for Building Airflow Network Modeling," U.S. Department of Energy, Washington, 1989.
- [14] *ASHRAE*, Atlanta, GA: American Society of Heating, Refrigerating and Air-Conditioning Engineers, 2001.
- [15] W. D. Walton, D. J. Carpenter and C. B. Wood, "Zone Computer Fire Models for Enclosures," in *SFPE Handbook of Fire Protection Engineering*, 4th ed., Quincy, Massachusetts: National Fire Protection Association, 2008, pp. 3-222 - 3-228.
- [16] *NFPA 101*, 2012 ed., Quincy, MA: National Fire Protection Association, 2012.
- [17] *NFPA 5000*, 2012 ed., Quincy, MA: National Fire Protection Association, 2012.
- [18] J. Hanke, A. Reitsch and P. J. Dickson, Newton, Massachusetts: Allyn and Bacon, Inc. , 1984.
- [19] *Experimental Statistics*, Washington, D.C.: U.S. Government Printing Office, 1966.
- [20] "Fire Casualties Study," in *Annual Conference of Fire Research*, Washington, 1977.